Escola d'Enginyeria de Telecomunicació i Aeroespacial de Castelldefels
UNIVERSITAT POLITÈCNICA DE CATALUNYA

TREBALL DE FI DE CARRERA

TÍTOL DEL TFC: Modelling of Tree Scattering in Rural Residential Areas at 3.5 GHz

TITULACIÓ: Enginyeria Tècnica de Telecomunicació, especialitat Sistemes de Telecomunicació

AUTOR: Ferran Catalán Ruiz

DIRECTOR: Prof. Dr.-Ing. Thomas Kürner

DATA: 25 de març de 2011

Declaration

I certify that the work presented here is, to the best of my knowledge and belief, original and the result of my own investigations, except as acknowledged. Any uses made within it of the works of any author are properly acknowledge at their point of use.

Ferran Catalán Ruiz

Abstract

During the last 10 years, the interest to have an internet connection at home has grown up. In urban areas with a high density of population has installed the optical fiber, which provides internet acces to the users. Otherwise, the rural areas, with a low density of population, the optical fiber is not implemented, so it's proposed Broadband Wireless access (BWA).

The rural areas have high density of vegetation, not like the urban ones. So in the prediction for urban areas is not usual to include a vegetation model.

This tesis studies if the vegetation is an important parameter to take into account in the path loss prediction. It's analized how to model the trees and a group of trees and the effects of this model into the propagation of the wave. Furthermore, the path loss is computed using a ray-based propagation prediction tool, where mechanisms of propagation are considered. The scattering from the trees is modelled using Foldy-Lax multiple scattering theory and the scattering from other elements as terrain, streets and the buildings are modelled using Lambert approach.

In order to determine the propagation effects of vegetation and hence to improve the propagation prediction, this thesis compares the predictions with a measurement campaign conducted at Hetzwege, Germany, where a WiMAX system operating at 3.5 GHz provides broadband wireless access to the village.

Contact Information

Author:
Ferran Catalán Ruiz
E-mail: ferran.catalan@gmail.com

Supervisor:
Kin Lien Chee
E-mail: chee@ifn.ing.tu-bs.de
Institut für Nachrichtentechnik
Technische Universitt Braunschweig

Contents

List of Figures

List of Tables

Chapter 1

Theory review

In the first chapter, all the topics used to develop the project will be reviewed.

At the beginning of this chapter, the wave theory, the electric field, the magnetic field, propagation and properties of electromagnetic waves are described. Once the wave theory is reviewed, there is another review about how the mechanism of propagation of these waves are.

Finally, the different prediction models employed to define the path loss of the wave propagating are revised.

1.1 Electromagnetic waves

A wave is a disturbance that travels through space and time. There are two principal types of waves:

- Mechanical waves.
- Electromagnetic waves.

On these two types of waves there is a propagation of a disturbance, transmitting energy and a quantity of movement. A mechanical wave requires a solid, liquid or gaseous elastic medium to propagate. On the other hand, an electromagnetic wave takes the form of self-propagating waves in a vacuum or in a material medium, for example a coaxial cable.

1.1.1 Electric and Magnetic fields

Electric field

The field generated by any electrically charged object is called electric field. This field exerts a force on other electrically charged objects. This concept was introduced by Michael Faraday on 1831.

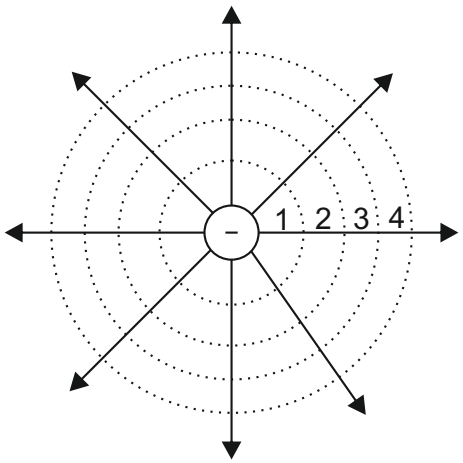

Figure 1.1. Electric field lines around one electrically charged sphere [1].

As can be seen in figure 1.1, the directions of the arrows show the direction of the force and each line around the sphere shows the electrostatic potential. There is a variation of potential depending on the distance from the sphere. The potential falls down as far as the distance from the object. Line number one has higher potential than line number four.

Magnetic field

The magnetic field appears when exists electrically charged with movement. Magnets have two types of pole, north and south pole and attract or repel one to another [1].

Figure 1.2 shows the lines of magnetic force around a wire, generated by moving charge and shows two types of poles with negative and positive signs.

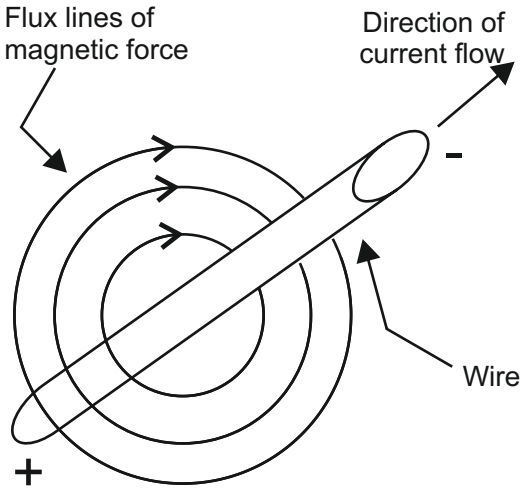

Figure 1.2. Magnetic fields around a current flow [2].

An easy way to determine the direction of the magnetic field from the electric field (see figure 1.3), is to use the corkscrew rule or right hand rule. The cork is the direction of the current flow and the lines of magnetic force will be in the direction of corkscrew rotation [2].

Maxwell's Equations

Maxwell's equations are a set of four equations[1] describing the electromagnetic phenomena. Maxwell 's work was to collect all the experimental results from Coulomb, Gauss, Ampere, Faraday and others [3, 4].

In 1864, Maxwell proposed a set of equations known as Maxwell's equations. Nowadays Maxwell's equations underlie the present radio propagation systems of telecommunications.

The four laws of Maxwell to describe the magnetic and electric field are [2]:

- Law 1: The electric field depends on stationary charges.
- Law 2: The magnetic field depends on moving charges.

[1] At the beginning Maxwell's equations were a group of 20 equations.

- Law 3: The electric field depends on a changing magnetic field.
- Law 4: The magnetic field depends on a changing electric field.

Maxwell's equations in vacuum

In vacuum, free of charge (charge density, $\rho = 0$) and free of current (current density, $J = 0$), all the equations are reduced to:

$$\nabla \cdot \bar{E} = 0 \tag{1.1}$$

$$\nabla \cdot \bar{H} = 0 \tag{1.2}$$

$$\nabla \cdot \bar{E} = -\mu_0 \frac{\partial \bar{H}}{\partial t} \tag{1.3}$$

These set of equations can be reduced to a simple equation of traveling where the directions of the electric and magnetic fields are perpendicular to the direction of travel and to each other.

$$c = \frac{1}{\sqrt{\mu_0 \epsilon_0}} \tag{1.4}$$

The combination of electric fields and magnetic fields is propagated through the space carrying energy at velocity c. In order to know the speed in vacuum, the electric permittivity value and magnetic permeability value are necessary to solve the equation 1.4 [5].
The electric permittivity in vacuum, in SI units:

$$\varepsilon_0 = 10^7/4\pi c^2 \tag{1.5}$$

The magnetic permeability in vacuum , in SI units:

$$\mu_0 = 4\pi 10^- 7 \tag{1.6}$$

Using the Maxwell's equation 1.4 it is possible to obtain the speed of light, usually denoted by c[2]:

[2]Speed of light in vacuum is denoted by c for the Latin *celeritas*, meaning "swiftness"

$$c = 299.792.458 m/s \tag{1.7}$$

1.1.2 Propagation of electromagnetic waves

The propagation of electromagnetic waves occurs with electric and magnetic components, that are inseparable. These two components are oscillating at right angles to one another and to the direction of wave [2].

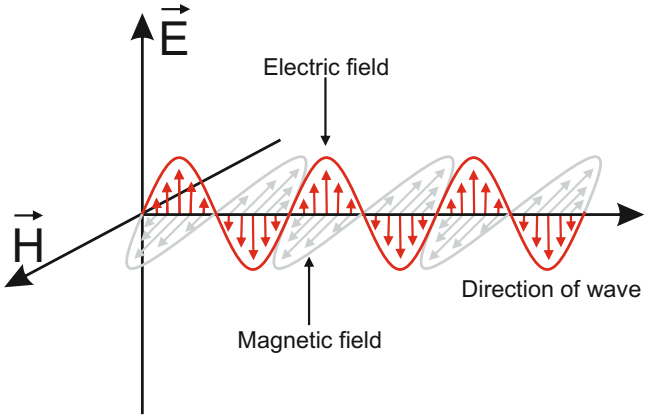

Figure 1.3. Propagation of one electromagnetic wave. The electric and magnetic fields are always at right angles to each other.

There are four laws (see section 1.1.1) that describe the electric and magnetic fields. These fields are traveling together through space in a wave form at the speed of light (see equation 1.7) and with different values of propagation described below in section 1.1.3.

Polarization

The polarization is a characteristic of electromagnetic waves and it indicates the plane which the wave is vibrating on. There is a convention where has been defined to take the electric component field as the polarization plane. There are three different types of polarization: circular, linear and elliptical, in its turn, vertical and horizontal are divided in lineal polarization that is most used.

The polarization of electromagnetic wave is an important characteristic of the wave because the transmitter and receiver antennas are sensitives to polarization [1].

1.1.3 Wave properties

In this section, the basic properties of an electromagnetic wave are discussed [2]. Figure 1.4 shows all these properties.

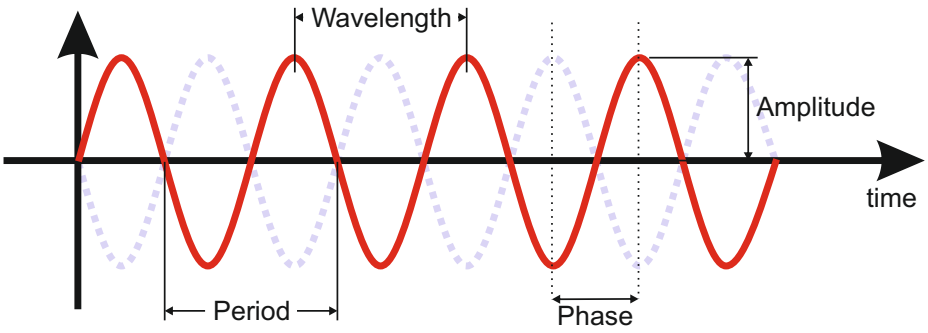

Figure 1.4. Different properties that define how a wave is.

Frequency

Frequency, written as f, is the number of oscillations completed in one second. As seen in figure 1.4 the period, written as T, is the duration of one oscillation in unit of seconds.

$$f = \frac{1}{T} \tag{1.8}$$

The relation between period and frequency is given in equation 1.8, the unit of frequency is Hertz and the unit of period is seconds [1].

Wavelength

The wavelength can be obtained by equation 1.9 with the speed of propagation and the frequency values.

$$\lambda = \frac{c}{f} \tag{1.9}$$

The wavelength is the distance over two consecutive maxims of the wave (see figure 1.4). A wave is traveling at constant speed c and a specific frequency f it is possible to get the wavelength by the equation 1.9.

When one wave impacts on an obstacle, the mechanism propagation depends on the obstacle size and the wavelength. If the surface of the obstacle size is not larger than the wavelength appears scattering but appears other mechanism of propagation [6].

Poynting vector

The poynting vector is the amplitude and direction of the power carried by the wave. Using equation 1.10, it is possible to obtain the power density, measured in W/m^2.

$$P = E \times H \tag{1.10}$$

The expression of real power transported by the wave is shown in equation 1.11. It represents the average value of the Poynting vector [6, 7].

$$P_{avg} = \frac{E_0 \cdot H_0}{2} \tag{1.11}$$

Phase

When there are two waves both depends one each other. Phase is the time difference between two electrical signals that oscillate at the same frequency. As can be seen in figure 1.4 there is a second gray wave in anti-phase[3] with the red curve.

1.2 Propagation Mechanisms

Electromagnetic wave is propagated through a medium by reflection, refraction, diffraction and scattering mechanisms. It depends on the frequency of the wave also the medium, the form and material where the wave impacts [8, 9].

[3]Anti-phase refers to a difference of 180 degrees (π radians). For equal amplitude the cancellation is possible.

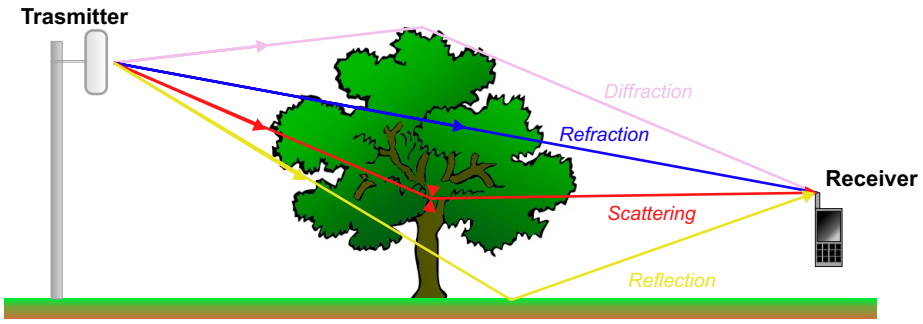

Figure 1.5. Different propagation mechanisms on a tree.

All propagation mechanisms showed in figure 1.5 are described in more detail below.

1.2.1 Refraction and Reflection

The refraction is the change of direction when one wave or ray comes from one medium to another. This effect appears when the wave impacts at an angle other than 90^o over the medium's separation and these mediums have different refraction index.

As seen in figure 1.6, a typical example of this phenomenon occurs when a spoon is put in a glass of water, it looks like a broken spoon but it is just an optical effect because the rays impact from the air (refraction index, 1.00027897) to water (refraction index, 1.335)[4] and the spoon is not at an angle of 90^o with the watter.

The reflection is the change of propagation of one ray or one wave on a separation surface between two different mediums and then the incident ray or wave returns to the initial medium.

Also, an easy example, when someone looks at the mirror, it reflects the incident rays in the same order as they approach the mirror.

[4]Values obtained from www.refractiveindex.info at $0.5\mu m$ and 25^o.

Figure 1.6. Refraction of light between mediums with different refractive index.

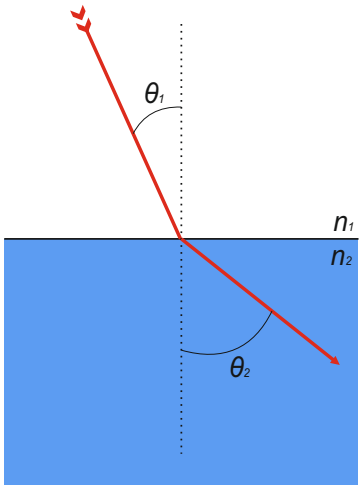

Figure 1.7. Refraction of light between mediums with different refractive index.

Snell's law

Snell's law, also known as law of refraction is a equation (see equation 1.12) to calculate the angle when one ray goes through the surface between two mediums with different refractive indices. Snell's law is described by,

$$\frac{sin\theta_1}{sin\theta_2} = \frac{v_1}{v_2} = \frac{n_2}{n_1} \tag{1.12}$$

Where v is the velocity in m/s, n is the refractive index (unitless) and θ are angles described in figure 1.7. As well, we can obtain the critical angle, where:

$$\theta_c = arcsin\frac{n_1}{n_2} \tag{1.13}$$

Any incident angle larger than critical angle may totally reflect in any medium with large refraction index.

Huygen's Principle

Reflection and refraction appear when the reflecting or refracting surfaces areas are larger than the wavelength of the radiation. When the surfaces areas are smaller than the wavelength of radiation then the behavior of the wave propagation is explained by Huygen's principle[5].

The principle suggests that when a wavefront encounters an obstacle or discontinuity, each point on a wavefront acts as the source of a secondary new waves and all these new waves combine to produce a new wavefront in the direction of propagation of the main wave [10].

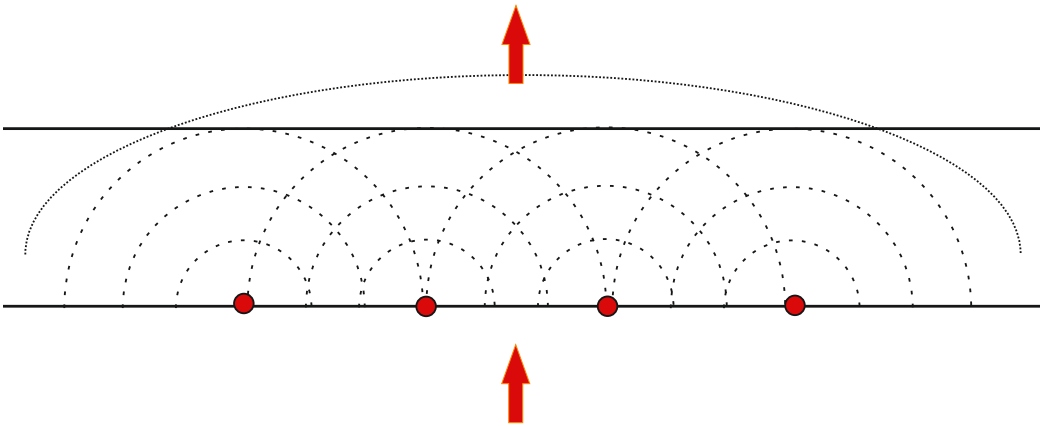

Figure 1.8. Huygen's Principle applied to the propagation of waves.

As seen in figure 1.8, the red dots indicate notional origins of new waves, refraction on an aperture in the manner of Huygens.

[5]Wave theory developed in 1678, and published it in his Treatise on light in 1690 by Huygen.

1.2.2 Diffraction

Diffraction phenomena occurs when waves encounter an object or a small overture and the direction of the waves change. This phenomenon makes that the useful signal can be behind obstacles.

When the propagation of waves encounter an obstacle, the phenomenon of diffraction allows a percentage of the signal to transfer around the obstacle. For example a receiver, behind a mountain or a big construction, can receive the signal from the transmitter situated to the other side of the obstacle.

Fresnel-zone ellipsoids

Fresnel zone is the space between the transmitter and the receiver of a electromagnetic wave. A group of ellipsoids exists around transmitter and receiver with a size of $n\lambda/2$ and n is an integer and depends on ellipsoid number.

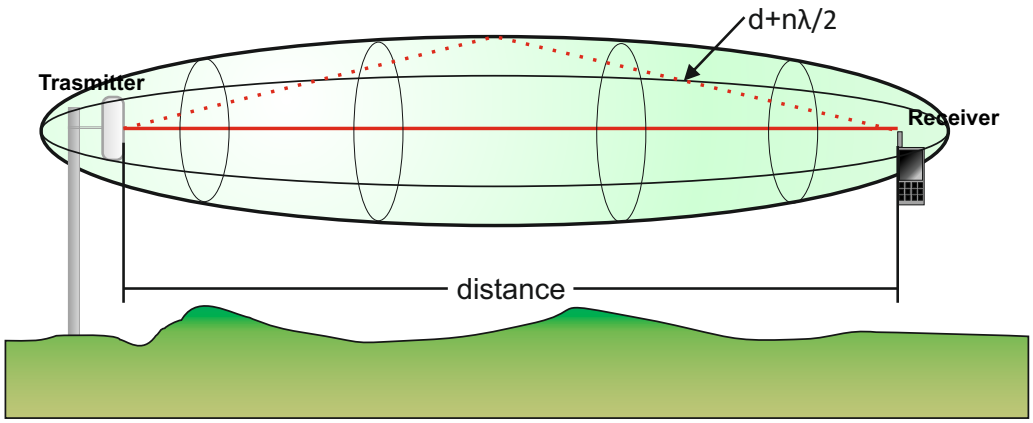

Figure 1.9. Fresnel zones.

In figure 1.9 is represented a transmitter and a receiver, a main red ray and the First Fresnel ellipsoid, the volume enclosed by this ellipsoid (n=1) is called the First Fresnel zone [8, 10].

Knife Edge Diffraction

Knife Edge Diffraction is a method to calculate diffraction loss. This method consists in an evaluation of all the obstacles that are in the first Fresnel zone.

Just in case of diffraction, all obstacles out the first Fresnel zone can be neglected [8].

When there are two or more obstacles the theory is extended from Single Knife-Edge to Multiple Knife-Edge Diffraction and mathematically the calculation begin to be complicated [8, 10].

There are several Multiple knife edge methods. Below, the main characteristics of some of them will be mentioned:

- **Bullington's equivalent knife-edge**: This method has the advantage of simplicity but some important obstacles are sometimes ignored.
- **Deygout method**: Used for a three obstacle path and the accuracy is highest when there is one dominant obstacle.
- **Epstein-Peterson method**: Following Bullington's method, Epstein-Peterson method fixes the limitation of the first method where some obstacles are ignored. The attenuation is calculated from one obstacle to immediately the next one, taking the first obstacle as virtual transmitter and the second as virtual receiver.
- **Giovanelly method**: A recursive method comparable with Deigout method.
- **Japanese method**: Similar concept to Epstein-Peterson method but the total path loss is computed as the sum of the losses.

All these methods can be used for path loss calculation but it is important to take into account that some algorithms to determinate the Multiple Knife Edge are complex and to obtain path loss predictions sometimes are too slow and sometimes are faster but the result is not enough accuracy. All these methods use correction equations after calculation.

1.2.3 Scattering

Scattering phenomena occurs in case of impact to a rough surface, the element has to be longer compared to the wavelength of the wave. After the incident, the wave is scattered in other directions [8].

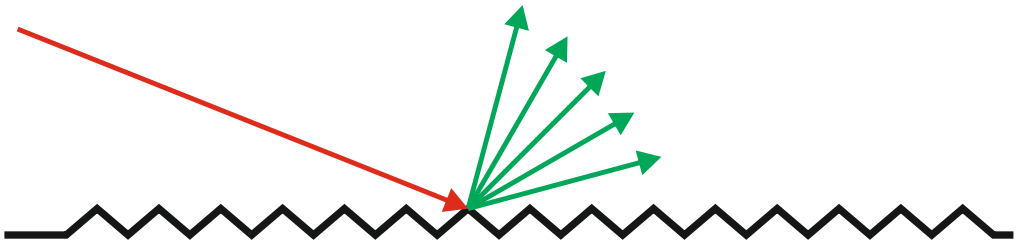

Figure 1.10. Scattering mechanism. There is a rough surface where a red ray means incident ray and the green rays mean the scattered rays radiating in other directions.

Scattering is incoherent when the phases are uncorrelated and random so the correlation length would be zero. Whenever the phases are correlated, coherent scattering appear.

There is other phenomena called *Dispersion* which makes the separations of the waves at difference frequency when crosses an obstacle. The most popular example is the rainbow which comes from the white light of the sun[6] is converted to all spectrum of lights when the white light impacts to the water drops in the air.

Kirchhoff approach

Kirchhoff's approach is a method that suits for slightly curved dielectric surfaces and has been used in the vegetation scattering study [8, 11]. This method should follow the requirement,

$$\begin{aligned} kl_c &> 6 \\ l_c^2 &> 2.76\sigma\lambda \end{aligned} \tag{1.14}$$

where k is the wavenumber, λ is wavelength, l_c is the correlation length of the surface and σ is the height standard deviation of the statistic surface.

[6]The light of the sun has all the range of visible light frequencies among others.

Lambert Model

For randomly rough surface, Lambert model is useful because it is very simple and easily to implement. This model is described by the following equation:

$$R(\theta_o) = \rho R_i \frac{1}{\pi} cos(\theta_o) \tag{1.15}$$

Where ρ is the surface reflection coefficient, R_i is the incident power and θ_o is the observation angle [7].

Foldy-Lax multiple scattering theory

Foldy-Lax scattering is a theory commonly used for the vegetation's scattering [12, 13]. All fields inside and scattered by a random medium are random functions of positions and can be divided into:

- **Coherent component**: Mean component.
- **Incoherent component**: Diffuse field or fluctuating component.

The coherent field for a plane wave that propagates inside the canopy of the tree is governed by the propagation constant K and is given by,

$$K = k + \frac{2\pi}{k} F^{eq}(\hat{k}_s, \hat{k}_i) = K' - jK'' \tag{1.16}$$

The equivalent scattering amplitude per unit volume of the canopy ($F^{eq}(\hat{k}_s, \hat{k}_i)$) is in general a complex number even for a lossless scatterer and it is related to scattering cross section, the specific attenuation is given by,

$$\alpha_c = 20K'' log_{10}e = 8.686\ K''\ (dB/m) \tag{1.17}$$

The incoherent scattered field intensity due to the tree canopy is

$$E_s^{inc} = \frac{E_i(d_1)}{\sqrt{4\pi} d_2} \sqrt{\sigma(\hat{k}_s, \hat{k}_i)} \tag{1.18}$$

Where d_1 is the distance between transmitter and the tree in meter, d_2 is the distance between tree and receiver in meter, $E_i(d_1)$ is the field incident on

the canopy coming from the transmitter and can be written as,

$$E_i(d_1) = \frac{\lambda}{4\pi d_1} e^{\left(-j\frac{2\pi}{\lambda}d_1\right)} \tag{1.19}$$

The bistatic cross section ($\sigma(\hat{k}_s, \hat{k}_i)$) on the entire canopy is given by,

$$\sigma(\hat{k}_s, \hat{k}_i) = \sigma^{eq}(\hat{k}_s, \hat{k}_i) I(\varphi_s) \tag{1.20}$$

Where $I(\varphi_s)$ describes which degree of each elemental canopy volume contributes to the total incoherent scattered field. Empirically, for a small K'', it can be approximated by,

$$I(\varphi_s) = \pi H R^2 \{1 + [K''R]^2(1 - cos\varphi_s)\} e^{\{-3.62K''R + 0.58[K''R]^2\}} \tag{1.21}$$

The equivalent scattering amplitude per unit volume of the canopy is given by,

$$F^{eq}(\hat{k}_s, \hat{k}_i) = \sum_{b=b_1,b_2,\ldots,b_{N_b}} \rho_b E\{F^b(\hat{k}_s, \hat{k}_i) + \rho_l E\{F^l(\hat{k}_s, \hat{k}_i)\} \tag{1.22}$$

Where ρ_b and ρ_l are the density of branches and leaves of the tree, respectively. Figure 1.11 shows the cross section for each element of one tree (branches and leaves) derived from the parameters from table 1.1 and with the equations 1.22, 1.16 and 1.17.

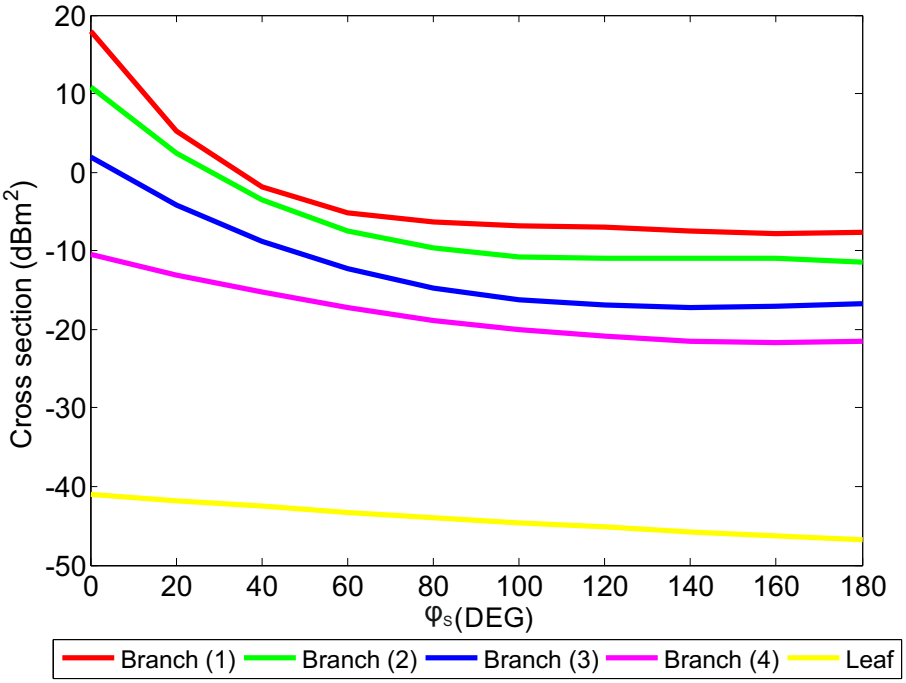

Figure 1.11. Mean scattering cross sections of branches and leaves. Where φ_s is the scattering angle between transmitter and receiver respect the tree, when $\varphi_s = 0$ the receiver is behind the tree respect the transmitter [12].

Scatterer type	**Radius (cm)**	**Length/ thickness (cm)**	**Relative permittivity**	**Density ρ (m^{-3})**
Branch (1)	11.4	131	$28 - j7$	0.05
Branch (2)	6.0	99	$28 - j7$	0.1
Branch (3)	2.8	82	$28 - j7$	0.7
Branch (4)	0.7	54	$28 - j7$	7
Leaf	0.37	0.02	$31 - j8$	500

Table 1.1. Size and dielectric parameters of branches and leaves [12].

The branches were divided into $N_b = 5$ groups depending to their radius and length.

Both figure 1.11 and table 1.1 are obtained from De Jong's work [12] but the density has been adapted to the local vegetation of this thesis.

At 3.5 GHz, the attenuation coefficient associated to the tree is of 1.51 dB and for defoliated trees (density of the leaves, $\rho_l = 0$) is 1.15 dB/m. A tree without leaves has a lower level of attenuation coefficient because the tree has less elements.

1.3 Path Loss prediction models

Prediction models to calculate the path loss can be divided into three groups, as shows figure 1.12 [14].

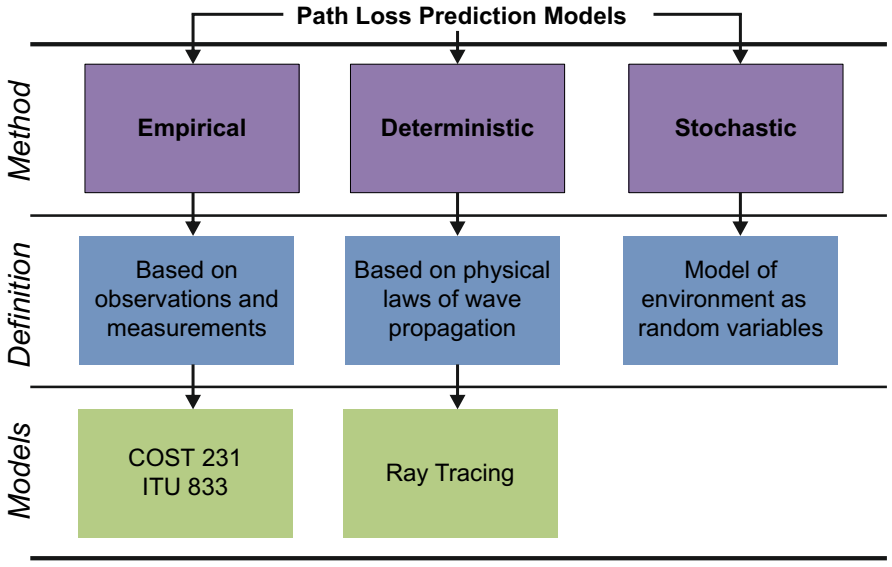

Figure 1.12. Path Loss models.

1.3.1 Empirical model

Sometimes it is not possible to make clear the wave propagation with an equation. The prediction is based on data obtained from measurements,

observations and average losses.

SEAMCAT (Extension of Hata model)

Okumura model is a radio propagation model guild with data collected in the city of Tokyo, Japan. Hata model can be used for frequencies up to 500 MHz.

The *European Cooperation in the field of Scientific and Technical research* (COST) 231 increase the frequency band from 500 MHz to 2000 MHz and the *Spectrum Engineering Advanced Monte Carlo Analysis Tool* (SEAMCAT) implement an extension from 2000 MHz to 3000 MHz. The extension of COST 231 and SEAMCAT Hata model includes correction terms for suburban and open areas [14, 15, 16].

1.3.2 Deterministic model

In contrast to empirical model, deterministic method is based on the physical laws of wave propagation to determine the received signal power, so that path loss can be obtained.

Ray tracing

Ray tracing is a method to calculate the path of the waves through or around objects. When the waves are traveling from the transmitter to the receiver, sometimes, is not possible to have a direct ray because in the middle of the link there are some objects which change the wave direction.

How the rays change depends on the properties and form of the object and the ray. Ray tracing works using the propagation mechanisms reviewed in section 1.2. This method is based on physical laws and it is possible to obtain parameters like path loss, incident angle, number of receiver rays, delay, distance, so on and so forth, depending on the developed software.

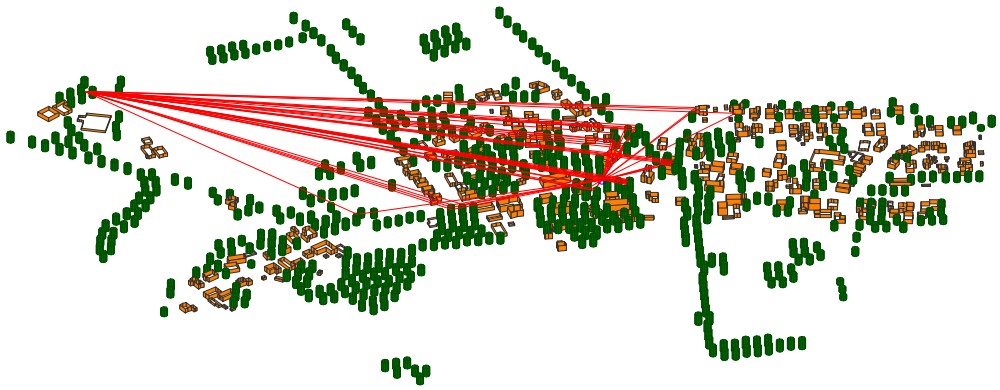

Figure 1.13. Ray Tracing from transmitter to receiver with 41 rays plotted. There are different propagation mechanisms around the trees, houses, streets and ground.

This method can be developed to run by reflected, penetrated, scattered or diffracted rays and with 2D or 3D data with information about the objects, buildings, streets, trees and ground.

1.3.3 Stochastic model

On the other hand, Stochastic models model the environment as a series of random variables. In favor of this method, it required minimum information but it generates path loss results with low accuracy.

Chapter 2

Vegetation model

To quantify the vegetation loss using a simulator tool, it is necessary to create a model of vegetation. The vegetation will be modeled as a group of trees, the sizes and the density can be changed to study different scenarios possibles.

The main objective of this chapter is to study some previous works about the vegetation modeling in order to predict the attenuation using a ray tracer simulator tool.

2.1 Previous work

The vegetation model is based on the multiple scattering theory of Foldy, Lax and Twersky. The tree is considered as a group of branches and leaves. Moreover they developed the theory of scattering from a manifold of objects assumed to have an arbitrary configuration.

2.1.1 Tree modeling

Trees are modeled as an ensemble of leaves and branches, having a random situation, orientation and distribution. This ensemble is random in space and time but commonly, it is assumed to be time-invariant.

As shown in figure 2.1, the tree canopy is modeled as a finite cylinder defined by the radius R and the height H. The origin of the coordinate

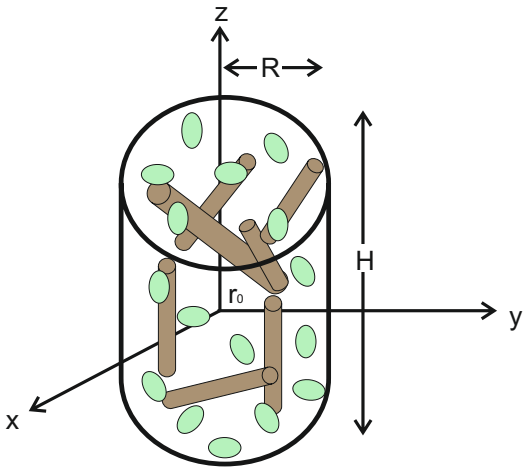

Figure 2.1. Model of tree as a group of branches and leaves inside a cylinder. The branches and the leaves are in a random situation, orientation and distribution.

system is located at the centre of the canopy r_o. The canopy cylinder contains branches and leaves. Also the size categories of the branches and the density of the branches and the leaves are taken into account.

The model of the tree canopy is an ensemble of leaves and branches inside a cylinder. Leaves are modeled as a lossy dielectric thin disc (see figure 2.2 (a)) and branches are modeled as a lossy dielectric thin cylinder (see figure 2.2 (b)).

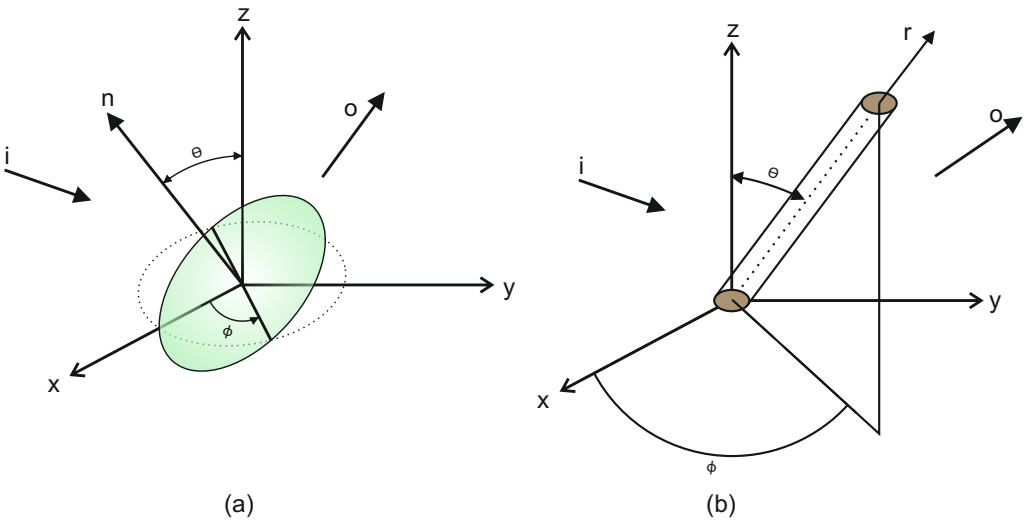

Figure 2.2. Leaf(a) and Branch(b) model.

Tree branches area composed of different tissue layers and all of them have different permitivity but are modeled as an homogeneous dielectrics complex permitivity. The cylinder direction is defined by an angle θ with respect to the z axis and an angle ϕ with respect to the x axis. The orientation of the larger branches was observed to be predominantly vertical and the leaves have no preference orientation at all.

Foliage leaf material is formed by a group of many cells of complex position and typically the layer thicknesses are smaller than the wavelength. As is shown in figure 2.2, the orientation of the disc is defined by the angle θ from the z axis and an angle ϕ from the x axis [12, 13, 17, 18].

2.2 Constructing a single tree model

In order to find an approach to model a tree, it is necessary to know the characteristics of one tree, which parameters can define a tree. This model has to be composed for faces[1].

2.2.1 Tree parameters

From a measuring Guide [19], it is possible to obtain three fundamental parameters that are necessary to define a tree. These parameters are:

- **Trunk circumference**: It means the diameter of the trunk. The trunk is measured, excluding dead branches, up from 4 feet or 1.22 meters from the ground.
- **Vertical tree height**: The height from the ground up to the top of the tree.
- **Average crown spread**: The most wide distance between two points of the extended crown.

With these parameters it is possible to define a tree but at this time, a new parameter will be used:

[1]The raytracer simulator needs to work with models constructed by faces.

- **Vertical trunk height**: Should be necessary to know how long is the height of the trunk without any branch or leaf. It's measured from the ground up to the first branch.

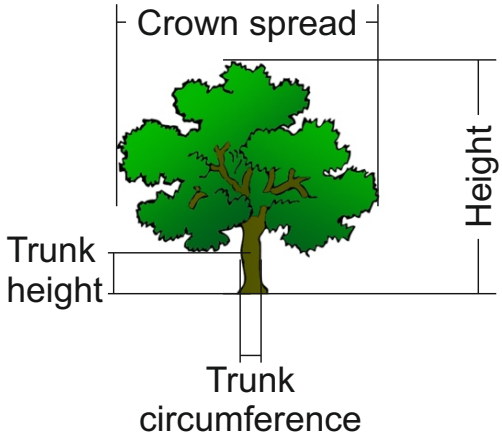

Figure 2.3. Parameters to define tree size: trunk height, trunk circumference, crown spread and height.

2.2.2 Tree model

Due to the fact that the simulator has some limitations, for example it works with object composed of faces, is not possible to design a model based in some previous works [12, 18].

Having known the basic parameters, that are necessary to define a tree, it is necessary to add these parameters, and all of them have to be available to modify in order to create different scenarios.

A tree model is created with two cylinders, one of them should represent the canopy, and the other one, should represent the trunk (figure 2.4 (b)). Finally, a composition of the two cylinders will be enough to create a tree model (figure 2.4 (c)).

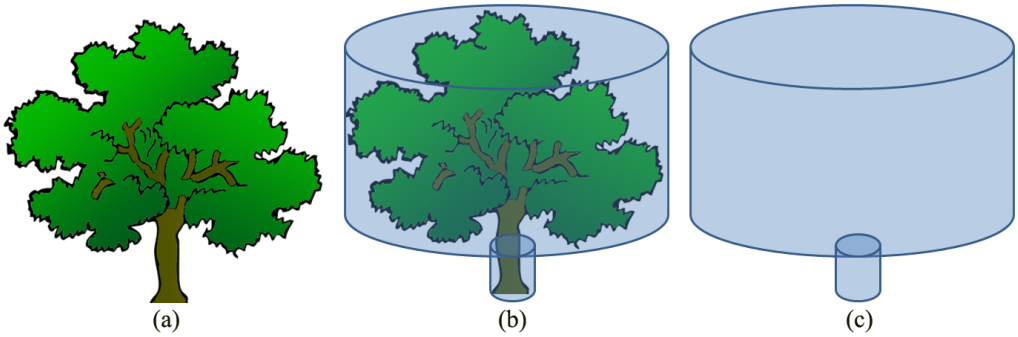

Figure 2.4. Main tree model idea

A cylinder can be approximated with a polygon, the maximum similitude with a cylinder will be determined by the number of faces chosen to build the polygon. As more faces of the polygon, it has more similitude with a cylinder.

2.2.3 Drawing one tree model

Some knowledge about trigonometry is required before drawing a polygon for the tree model. To draw a polygon, it is necessary to have information about the following parameters:

- Radius of the circumference.
- Number of sides of the polygon.

Once all these parameters have been defined, the polygon can be drawn. In the first place a circumference has to be divided in N (number of faces of the polygon) with equal sides, then to evaluate the cosine and sine of every angle of every corner.

Each vertex will have the same difference of angle between two sides with the next vertex and the previous vertex. Each angle can be calculated with equation 2.1 in radians,

$$\theta(n) = (2\pi/N)n \tag{2.1}$$

where N is the number of faces and n is the vertex to obtain the angle.

Once the angle of each vertex from the center is calculated, using the equations 2.2 and 2.3 get the position of these points based on the radius of the polygon.

$$Coordenate\ X = cos(angle) \times radius \tag{2.2}$$

$$Coordenate\ Y = sin(angle) \times radius \tag{2.3}$$

Up to this point, the base has been built, the next step is to build the rest of the tree model. Using a tree height, the cylinder is created by the polygon base.

As shown in the figure 2.5, it is possible to construct cylinders of different sizes and numbers of faces.

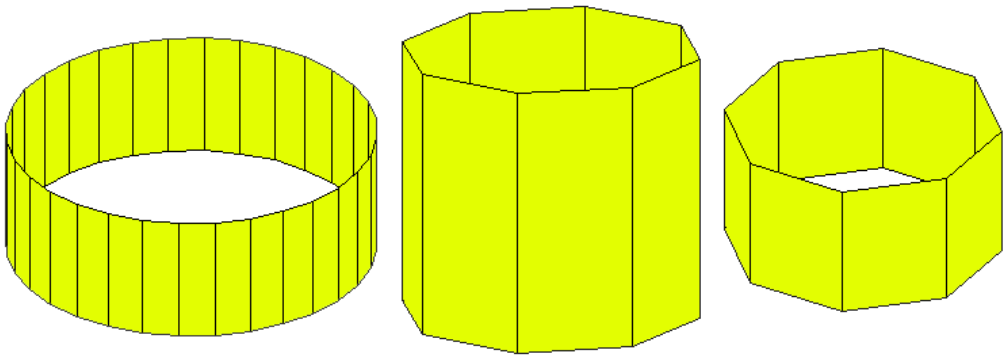

Figure 2.5. Different cylinders created by a polygon base

From the main tree model (figure 2.4), it is possible to create a tree model with two cylinder. Finally, a tree model has been built (2.6) and it can be defined by the following:

- Radius of the first and second cylinder.
- Number of faces of the first and second cylinder.
- Height of the first and second cylinder.

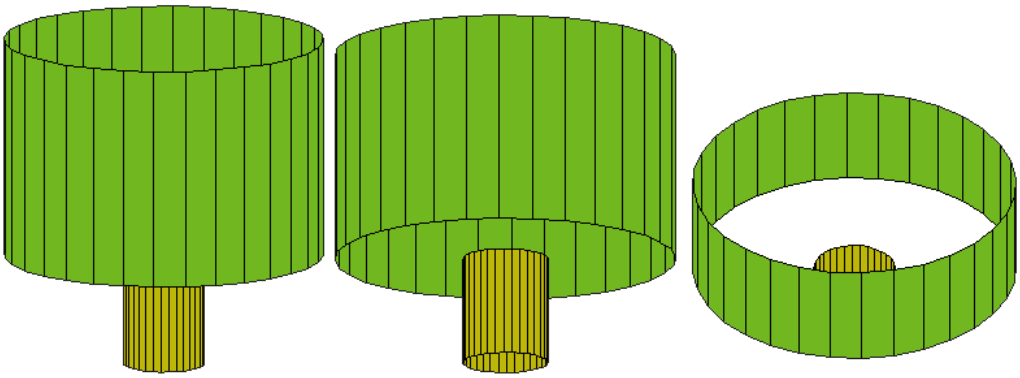

Figure 2.6. A tree model created by two cylinders of 32 faces each.

2.3 Building one group of trees

When a tree has been created, the next step is to know how to build a group of trees. In this section, density and distribution of the forest is studied, some parameters to be taken into account are: density measure and tree distribution.

2.3.1 Density measure

Often, ecologists measure density by the number of plants per unit area. But in a forest area it is difficult to apply directly the mean of the word "density" because an area with 100 knee-high seedlings per hectare is hardly as dense as a stand with 100 tall trees [20].

Basal area as a measure of density

In forest management the Basal Area (BA[2]) measure is often used. Usually this measure takes the trunk circumference (see chapter 2.2.1) of every tree, including the bark. Measures are usually made for 1 hectare. Individual basal area (BA_i) is calculated by,

[2]Basal area is the area of a given section of land that is occupied by the cross-section of tree trunks and stems at their base.

$$BA_i = \pi(\frac{d}{2})^2 10^{-4} \ [m^2] \tag{2.4}$$

$$D_f = \sum BA_i \ [density/hectare] \tag{2.5}$$

$$BA_f = \frac{D_f}{N} 100 \ [\%] \tag{2.6}$$

Where d is the Diameter at Breast Height (dbh[3]) in cm and N is the total number of trees. Equation 2.5 gives the density of a family of trees in one hectare of terrain (D_f) and equation 2.6 gives the density of family trees in percentage (BA_f) [21].

Stand Density index

The Stand Density index (SDI[4]) also called Reineke's Stand Density Index originally described as a measurement of relative density. The Stand Density index depends of two variables:

- Plant number.
- Plant size.

Reineke's SDI is calculated directly using equation 2.7 where is possible to obtain the number of trees per unit area with specific diameter, in this case $diameter$[5] $= 25.4 \ cm$.

$$SDI = N \left(\frac{D}{25.4} \right)^r \tag{2.7}$$

Where N is the number of trees per hectare and D is the diameter of the trunk. Parameter r must be different for each species and location although Reineke use parameter r as a constant $r = 1.605$ for all environment [22].

[3]Diameter at breast height (about 1.4 meters from ground)

[4]Founder of SDI, appears in 1933 Perfecting a stand-density index for even-aged forest. "Journal of Agricultural Research" 46:627-638

[5]Usually is used inches units. The conversion to inches, 25.4 $cm = 10$ $inches$

2.3.2 Tree distribution in the forest area

In relation to the spatial distribution of the trees, there are three classical theoretical models about how it is possible to find the distribution of the trees in a forested area:

Random distribution

As seen in figure 2.7 (a), the distribution of the trees is in random order.

Grouped distribution

As seen in figure 2.7 (b) the distribution of the trees is in groups of random nature.

Uniform distribution

As seen in figure 2.7 (c), the distribution of the trees is schematic. Between trees there is the same space of separation.

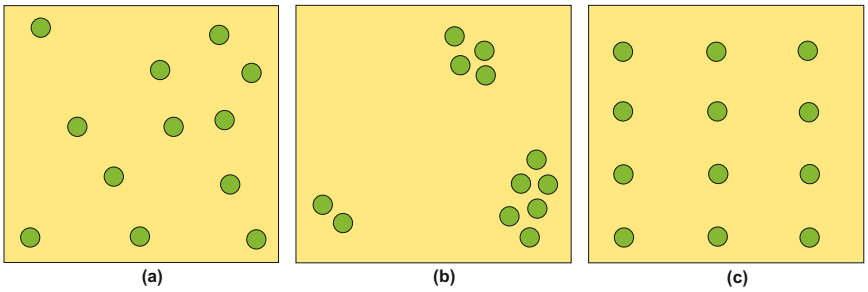

Figure 2.7. Distribution of the trees in a forest area

2.3.3 Drawing one forest model

As seen in section 2.3.1 there are some different methods and theories to calculate the density of the trees in a forested area. Assuming the vegetation is of same species, then it is possible to use directly the definition of density[6].

[6]Density is the amount per unit size

The density of a group of trees is calculated by the number of trees in an area of one square hectare[7].

$$density = \frac{n\ trees}{1\ hectare^2} \tag{2.8}$$

An other way to define the density of a forest can be the separation between trees. The separation can be obtained also by the density,

$$separation\ between\ trees = \frac{1}{density}\ (hectare^2) \tag{2.9}$$

Once the density of the forest is defined, the trees are placed on the surface of the vegetation area. The distribution of the trees has to be uniform to fill the whole possible area because the forest will be constructed in an area full of vegetation. Figure 2.8 shows some examples changing the diameter canopy and the tree separation in the forest.

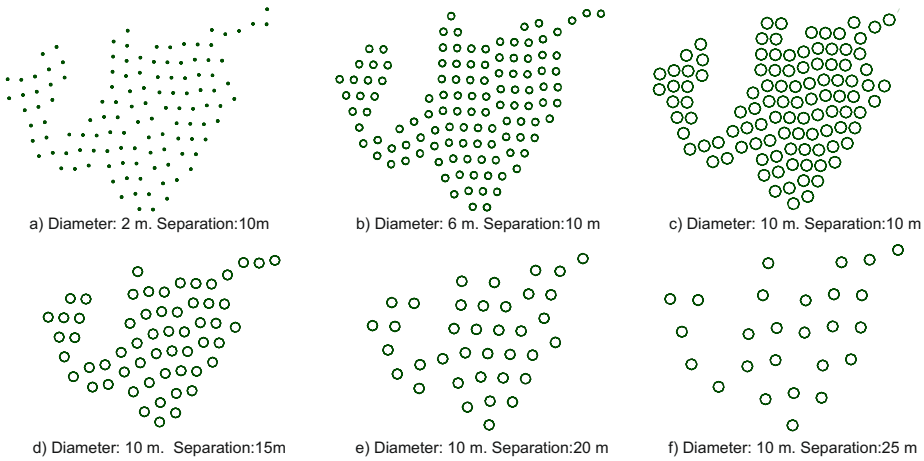

Figure 2.8. Tree distributions with different values of separation and diameter of the canopy. Diameters of the canopy changes from 2 meters up to 10 meters (figures a,b and c). Separation between trees changes from 10 up to 25 meters (figures d, e and f).

[7] 1 square hectare is equal to 10,000 square meters

The problem of limitation area

For the construction of a group of trees, it is possible to select different values of radius and separation between the trees. When the values are changing, it is important to respect always the vegetation boundary.

As a precautionary measure of this situation the boundary area has to be carefully taken into account in order not to cross these borders. For that has been followed a process at the moment to create a group of trees for each combination of separation and radius.

Whenever an area of vegetation is obtained where to place the trees, it is necessary to know the value of the radius because then the vegetation area will be trimmed around the perimeter. Figure 2.8 shows the trees inside the vegetation boundary for different combination of diameter and separation of trees.

2.4 Local vegetation

Once the tree model has been reviewed, the tree size has to be adjusted to the local vegetation to obtain the maximum possible similarity as compared to a real situation. In this thesis, the vegetation in Hetzwege[8] will be analyzed.

2.4.1 Tree model

Throughout all area of Hetzwege, there are different types of trees, some examples are given in figure 2.9.

[8]Hetzwege is a small village in the country of Rotenburg (Wümme), Germany

Figure 2.9. Diversity of trees grown in Hetzwege village. Diversity of trees: Oak (a), Birch (b) and Chestnut (c) [Clip art by karenswhimsy.com].

Properties of the canopy

Table 2.1 shows the parameters that define the canopy and the trunk of a oak tree [23].

Properties	Canopy	Trunk
Permitivity	29.1204	12.9844
Loss tangent	0.2783	0.3261

Table 2.1. Properties of the tree.

2.4.2 Model of a group of trees

When there is more than one tree, the separation between trees (see equation 2.9) is taken into account.

Separation between trees

To choose the separation between trees, it is important to know the radius of the canopy. The separation between trees will never be less than the diameter of the canopy because in case of selecting a separation smaller than the canopy diameter, it means that the canopy of the trees overlap.

This parameter will be the same for all vegetated area. The area of vegetation will be full of trees depending on the density selected (see equation 2.8).

The distribution of a group of trees is modeled as uniform distribution because in the map are located the vegetation area, thus all this area has to be full of trees and uniform distribution is the best option to have an area full of trees.

2.4.3 Drawing local model vegetation

In order to create a model of the village of Hetzwege, information about the environment is provided as follows:

- Pixel map with clutter types information (see figure 2.10)
- Coordinates of every pixel
- Height of the trees

In the first map there is the clutter that compose the model of the village. Each element is represented by a number and it's plotted in different colors (see figure 2.10).

Element	Number	Color
Ground	0	blue
Streets	1	cyan
Vegetation	2	yellow
Houses	3	red

Table 2.2. Different elements in the environment of Hetzwege.

Joining the pixel map (see figure 2.10) and the coordinates map can be obtained a resolution[9] of 3.3 meters for eastern component and 2 meters for northern component.

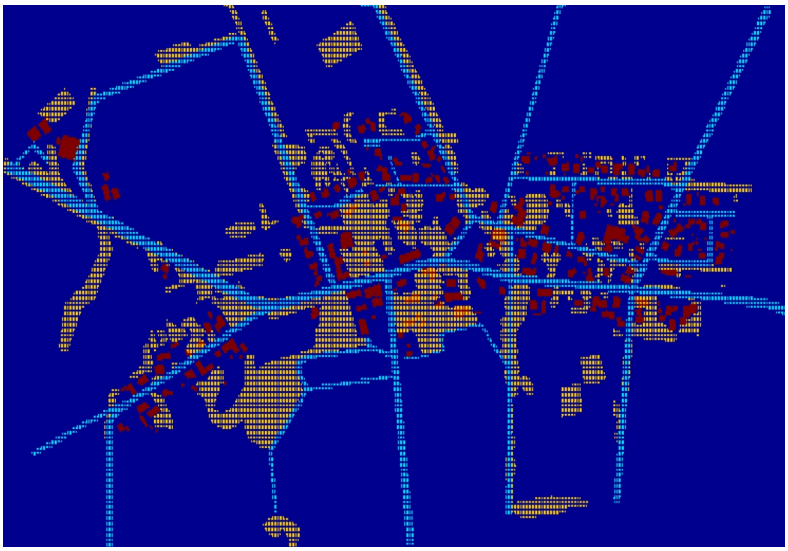

Figure 2.10. Pixel map of Hetzwege with clutter information.

The coordinates of each corner of the pixel map have been marked into an aerial image of the region (figure 2.11). All area inside the square, drawn in this figure, is the area to model.

[9]The quality of being resolute.

Figure 2.11. Aerial photography of modeled area [Image obtained from google.maps.com].

Following previous investigation, a model of the terrain, houses and streets is given. This model is presented in figure 2.12 and it has to be completed with the vegetation model.

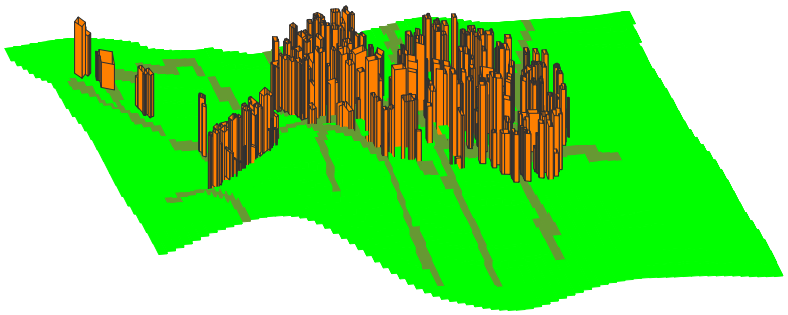

Figure 2.12. Scenario with real size ground and house in 3D.

The position of the trees is depending the value of diameter and separation of the trees. For this map, the distribution selected is uniform and to obtain the position of the trees is necessary to know all area where can be a tree. As can be see in figure 2.13, all blank spaces near a vegetation pixels are change to a vegetation pixel.

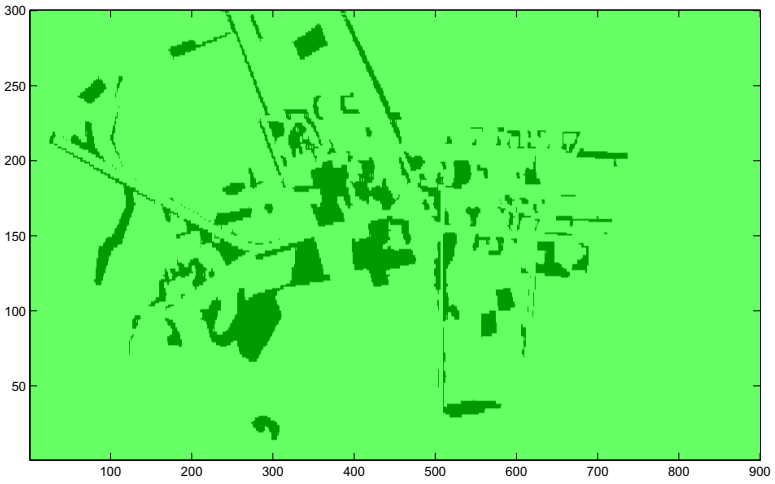

Figure 2.13. New vegetation area obtained from the original data.

Figure 2.14 shows a 3D map for a group of trees modeled with polygon of 8 faces, diameter of canopy of 6 meters and separation between trees of 10 meters (see more top view examples for polygon of 8 faces in appendix C).

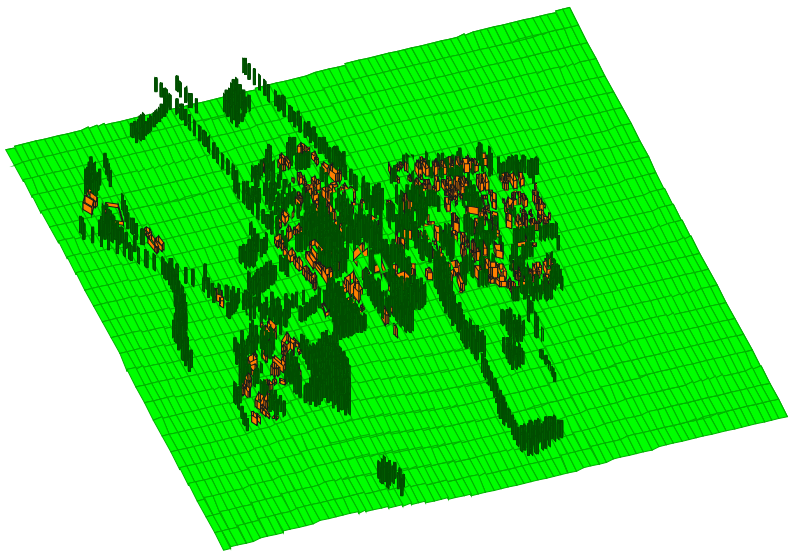

Figure 2.14. Scenario with the ground house and trees of 6 meters of diameter and 10 meters of separation between trees.

The process to create a group of trees from a clutter map can be seen in appendix A. This process describes step by step, functions, input and output parameters needed to obtain the final model of a group of trees.

Chapter 3

Simulations

This chapter describes how the path loss is predicted using ray tracing simulator tool. Also, are described the configuration used for the simulator tool.

In order to analyze different combinations of a group of trees model, the simulations have been run with different maps. The maps are defined by the group of trees model which can be modeled in function of the number of faces of the polygon, diameter of the canopy and separation between trees.

3.1 Ray-tracer simulator

As shown in section 1.3.2 ray-tracing is a deterministic model to determine the path loss of the wave propagation based on the physical laws of wave propagation.

3.1.1 Configuration

Table 3.1 shows the settings to specify which propagation mechanisms are used. If the number of reflections rays is increased, the simulation takes long time.

Parameter	Value
Number of reflections rays	1
Reflection propagation	Switch on
Scattering propagation	Switch on
Diffraction propagation	Switch off
Scattering type	Lambert type
Number of scatter rays from a plane	1

Table 3.1. Parameter's settings for Ray-tracer simulator.

Also, some information about the transmitter and the receiver is needed to run the simulator.

- Transmitter and receiver position (x,y,z)
- Transmitter and receiver orientation (theta, phi)
- Frequency and power from the transmitter

The base station has been situated on a mast of 25 meters. The antenna operates at 3.5 GHz with a gain of 23 dBi and a power of 3.2 W. The effective power transmitted by the antenna can be calculated as,

$$Power\,transmitted = 10log_{10}(3.2 \times 1000) + 23 = 58\ dBm \tag{3.1}$$

3.1.2 3D File

As shown is section 1.3.2 a ray-tracer simulator can be developed with 2D and 3D data. In this thesis, the simulator works with 3D data (file format defined in figure 3.1). This file contains information about the ground, houses, streets and vegetation of the village.

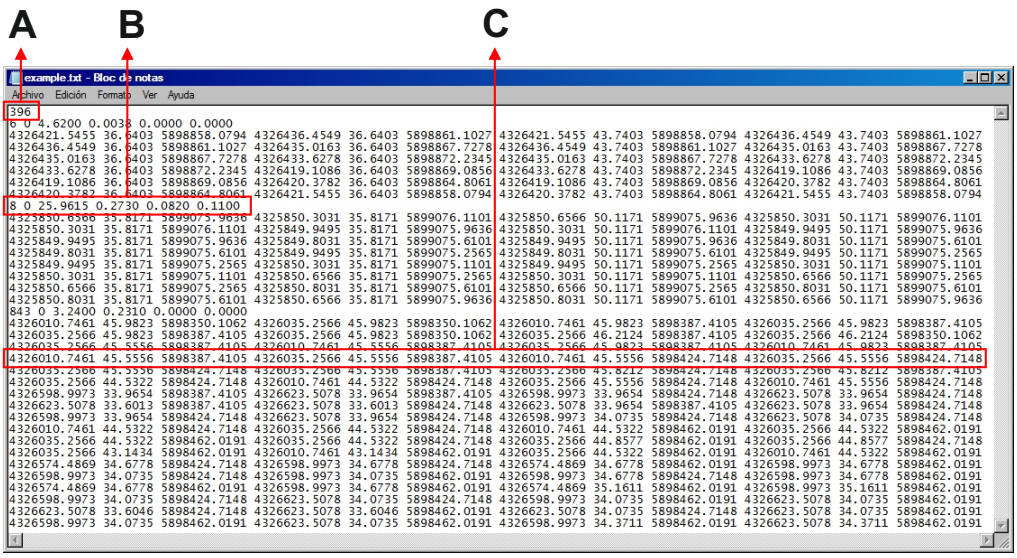

Figure 3.1. File 3D example to load on ray-tracer simulator.

Figure 3.1 is an example of a file ready to be loaded into the Ray-tracer software. The first line is defined as the total number of objects (area A from figure 3.1).

The first object shown in this example is a house of six planes, the second object is a tree of eight planes and finally the ground composed of eight hundred forty three planes. Also, the input file describes the characteristics of the object that is going to be drawn (area B from figure 3.1).

- First position: Number of faces of the object
- Second position: Ground plane
- Third position: Permitivity
- Fourth position: Loss tangent
- Fifth position: Correlation length of the surfaces
- Sixth position: Height standard deviation of the static surfaces

Area C shows the coordinates in Gauss-Kruger of every corner of the plane. To define a plane, the order of the corners is important. In figure 3.2 the order of corners is defined.

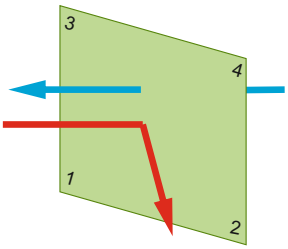

Figure 3.2. Order to define a plane in 3D file.

When a plane is defined it has to be written in the order described in figure 3.2. The arrow shows what is happening with a ray coming from the front of the plane (red ray) and a ray coming from the back of the plane (blue ray). In the case of red ray, it is reflected, diffracted or scattered.

3.1.3 Output results

After simulation every ray arriving to the receiver point is saved in an array with the information shown in figure 3.3 where the transmitter, the receiver and the object, in this case a tree, can be identified.

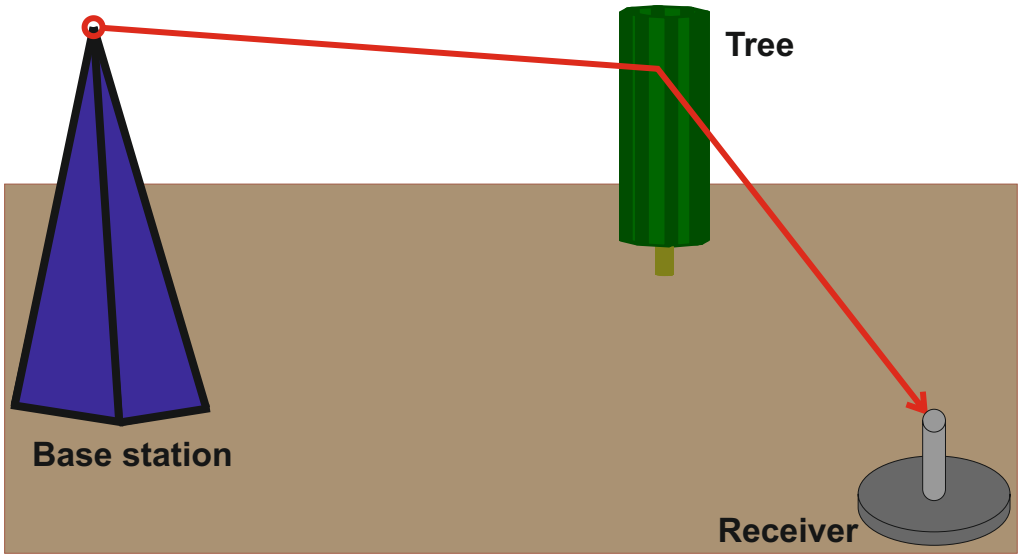

Figure 3.3. Information obtained by ray tracer simulator.

Apart from the position of each element, simulator gives other interesting

information such as: delay, distance, real received power, imaginary received power, path loss (for a transmitter power of 0dB), angle of arrival in azimuth, angle of arrival in elevation, angle of departure in azimuth, angle of departure in elevation and information about the type of propagation's mechanism that has been considered. The different types of propagation are: direct ray, reflection,Lambert, diffraction or Kirchhoff scattering.

Ray tracer simulator gives for each receiver position an array of rays and each one of them contain all information presented before.

In this thesis more information will be added because some parameters are necessary during the estimation of tree scattering. The incorporation of data is explained in the following section 3.2.

3.2 Processing obtained data

Once the simulations are finished, receiver rays scattered from trees will be analyzed using Foldy Lax multiple scattering theory (see section 1.2.3).

3.2.1 Process to analyze scattered rays

Following De Jong's work [12] the incoherent scatterd fields from trees is derived using Foldy Lax multiple scattering theory and so extra information is needed.

Extra information which contains the center position of the tree, the height, the number of faces, the position of each tree are needed to derive the incoherent scattered field.

For every point ray tracer gives an array of rays, each of them is analyzed as follow below,

- Check if the mechanism of propagation is scattering.
- Check if the reflection plane belongs to a tree.
- Modify scattered field using Foldy-Lax equations for scattered tree rays (see section 3.2.2) and take into account one ray per tree.

3.2.2 Scattered field for vegetation

In this thesis, the incoherent scattered field of the vegetation is modeled using Foldy-Lax multiple scattering theory and the information obtained from the ray-tracing is modified with the aim to use the equations shown in section 1.2.3.

For each ray scattered on a tree, the angles and distances between base station, tree and receiver are calculated again because the scattering is calculated at center of the canopy (center of the tree volume). The information about the center of the tree volume is obtained by the class called *Forest*[1].

Figure 3.4 shows the top view of figure 3.3 and with white dotted line represents the new triangle that it is marked over the old scattered ray from Lambert approach.

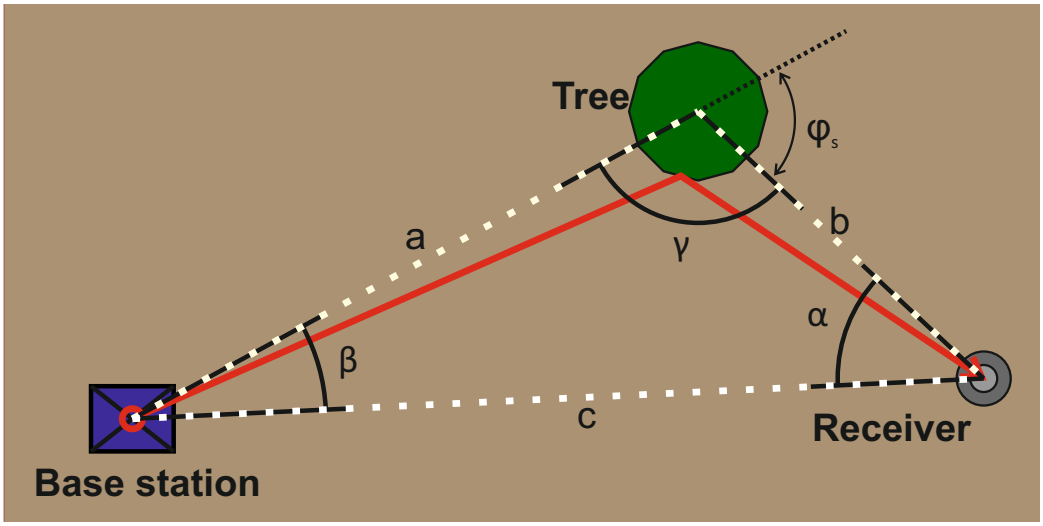

Figure 3.4. Angles and distance of ray's path. Base station to tree and tree to receiver.

Every distance shown in figure 3.4 can be obtained using trigonometry,

$$a = \sqrt{\frac{a^2 - b^2 - c^2}{-2bc}} \tag{3.2}$$

[1] *Forest* is a class with information about every tree created in the scenario. See appendix B for more information about this class.

$$b = \sqrt{\frac{b^2 - a^2 - c^2}{-2ac}} \tag{3.3}$$

$$c = \sqrt{\frac{c^2 - a^2 - b^2}{-2ab}} \tag{3.4}$$

and also the angles by,

$$\alpha = \arccos\left(\frac{b^2 + c^2 - a^2}{2bc}\right) \tag{3.5}$$

$$\beta = \arccos\left(\frac{a^2 + c^2 - b^2}{2ac}\right) \tag{3.6}$$

$$\gamma = \arccos\left(\frac{a^2 + b^2 - c^2}{2ab}\right) \tag{3.7}$$

then, equation 1.21 is implemented by,

$$Radius\ R = \frac{diameter\ canopy}{2} \tag{3.8}$$

$$Height\ H = height\ tree\ position + \left(\frac{height\ tree}{2}\right) \tag{3.9}$$

$$Angle\ \varphi_s = \pi - \gamma \tag{3.10}$$

Where φ_s is the scattering angle.

At the moment to create the group of trees model, the diameter of the canopy is defined. The height and position of the trees are different for every tree and it is obtained from the class *Forest*.

The cross section of every element of the tree canopies (see figure 1.11) is associated to a density with the aim to obtain the attenuation coefficient of the entire canopies. Table 3.2 shows the densities used during the simulation and the total attenuation associated for winter predictions and summer predictions. In winter predictions, the total coefficient for the tree (defoliated trees ($\rho_l = 0$)) is 1.15 dB and in summer predictions, the total coefficient for the tree is 1.51 dB

Scatterer type	ρ **Summer** (m^{-3})	α_c **Summer (dB/m)**	ρ **Winter** (m^{-3})	α_c **Winter (dB/m)**
Branch (1)	0.05	0.15	0.05	0.15
Branch (2)	0.1	0.11	0.1	0.11
Branch (3)	0.7	0.29	0.7	0.29
Branch (4)	7	0.6	7	0.6
Leaves	500	0.36	0	0
Total		1.51		1.15

Table 3.2. Attenuation coefficients associated with branches and leaves at 3.5 GHz

3.2.3 Dominant rays (Scattering vs. Diffraction)

Diffraction mechanism is not considered in ray-tracer simulator tool because is difficult to define diffraction with rays. Diffraction loss are calculated with Deygout diffraction method and it is included the extension of Hata model at 3 GHz by SEAMCAT with the aim to compare with Ray-tracer data. Both losses are compared and the dominant loss is taken into account [24].

3.3 Simulation of scenarios

For simulations, it is necessary to choose an optimum parameters because in one hand we need to run a quick simulation and on the other hand we need to obtain a good simulations values. For this reason, the trunks of the trees are neglected and the new tree model is one polygon constructed from the ground to the top of the tree as in [17].

Thus from now on, in this thesis, a group of trees model can be defined by the number of faces of the polygon, the diameter of the canopy and the separation between trees.

3.3.1 Scenarios

The simulations are divided into two groups. The first of the groups it is study the tree model behavior and the second group it is study the path loss accuracy of the predictions. Winter predictions are compared with winter measurements and summer predictions are compared with summer measurements.

There are 5434 different receiver points around the village to predict the path loss. The study of the group of trees model behavior is done with simulations of 500 points (see figure 3.5) and combinations of scenarios from table 3.3. These points habe been selected because are inside and outside of the center of the village. The path loss accuracy of the prediction is done with all 5434 receiver points and with the scenarios shown in table 3.4.

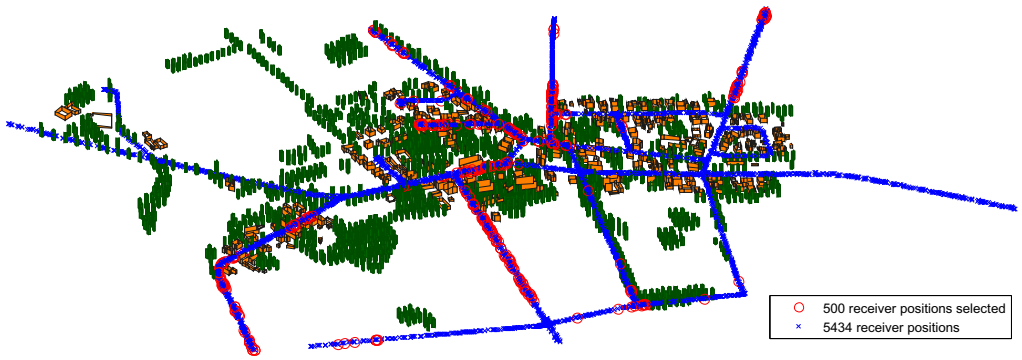

Figure 3.5. Receiving points used to analyzes tree model behavior. The blue crosses are the receiver positions around the whole area and the red circles are the 500 receiver positions selected of 5434 points to the study of the group of trees model behavior.

Different scenarios have been created, by varying the parameters of the group of trees model. The group of trees have been modeled with all possible combinations of different polygon's face, diameter of the canopy and separation between trees, these values are shown in table 3.3. In total, 80 different scenarios have been simulated.

Parameter	Values
Faces	6, 8, 12, 16
Diameter of the canopy (meters)	2, 4, 6, 8. 10
Separation between trees (meters)	10, 15, 20, 25

Table 3.3. Combination of scenario used during the simulations I.

Parameter	Scenario 1	Scenario 2	Scenario 3	Scenario 4	Scenario 5	Scenario 6	Scenario 7	Scenario 8	Scenario 9	Scenario 10	Scenario 11
Number of faces	8	8	8	8	8	8	8	8	8	8	8
Diameter of canopy (m)	2	6	6	6	6	10	10	10	10	20	20
Separation between trees (m)	20	10	15	20	25	10	15	20	25	10	15

Table 3.4. Combination of scenario used during the simulations II.

All data obtained have been saved as shown in figure 3.6 in files of 100 points with the aim to have small sizes of data of each file.

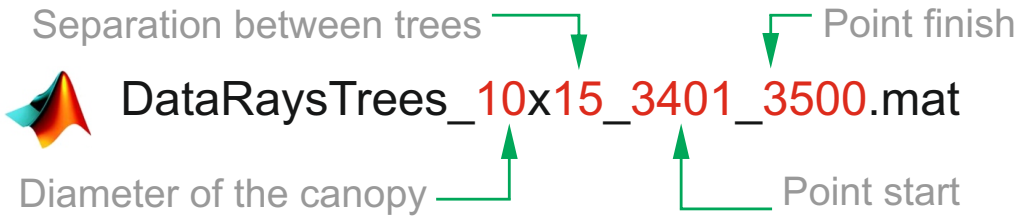

Figure 3.6. File format to data saved.

3.3.2 Measures to obtain

The behavior of the group of trees is analyzed as follows:

- Trees.

  Number of trees that has been constructed into the scenario depending on the radius and the separation between trees.

- No rays.

  Sometimes no ray arrives at the receiver (see section 2.3.3). This parameter indicates the number of points where no ray is received at the receiver.

- Direct ray.

  This parameter indicates the number of receiving points where there is a direct line-of-sight from the base station.

- Mean of rays.

  The average number of ray received at the receiver.

- Mean of tree scattered rays .

  The average number of ray scattered on a tree received at the receiver.

The accuracy path loss prediction will be evaluated using the mean error, the standard deviation and the Root Mean Square prediction error (RMS).

- Mean error.

  The mean error compares the prediction from simulations with the measurements data, for winter and summer season. Mean of error is calculated by,

  $$\bar{X} = \frac{1}{n}\sum_{i=1}^{n}(|L_{m_i} - L_{s_i}|) \tag{3.11}$$

  Where L_m is the path loss measurement value at ith position point, L_s is the path loss predicted value at ith position point and n is the number of receiver points [25].

- Standard deviation.

The standard deviation is a dispersion measure used for probability theories and statistics The standard deviation is calculated by,

$$\sigma = \sqrt{\frac{1}{n-1}\sum_{i=1}^{n}(X_i - \overline{X})^2} \tag{3.12}$$

Where n is the number of receiver points, X_i is the error for each receiver point at ith measurement point and $\overline{X}$ is the mean error of all points [25].

- RMS error.

  The Root Mean Square is a statistical measure of the magnitude of a varying quantify and it is calculated by,

$$X_{RMS} = \sqrt{\frac{1}{n}\sum_{i=1}^{n}X_i^2} \tag{3.13}$$

  Where n is the number of receiver points and X_i is the error for each receiver point at ith measurement point [26].

3.3.3 Path Loss prediction results

Winter measurements has not the same number of receiver positions like summer measurements because for every point of the measurements, it is compared with the receiver position. All points with a difference of situation higher than 6 meters have been neglected because the basic standard Global Position System (GPS) has an error of 3 to 6 meters when it is used in measurements [27]. Also every receiver position with any arrived ray is neglected.

All information about the prediction results is saved in files. The information saved is shown in table 3.5.

Variable name	Description
PL_winter	Propagation predictions in winter season.
PL_summer	Propagation predictions in summer season.
Info_winter	Analysis of the results for whole area in winter.
Info_summer	Analysis of the results for whole area in summer.

Table 3.5. Description of the file with the predictions results.

Every simulation run has the variables shown in table 3.5 which are explained in tables 3.6 and 3.7

Column number	Description
1	Eastern component of the receiver position.
2	Northen component of the receiver position.
3	Distance to the base station.
4	Path loss of measurements
5	Path loss of ray-tracing predictions
6	Position of the receiver point.
7	Area of the receiver points.
8	Path loss of diffraction predictions.
9	Path loss of SEAMCAT (Extension of Hata model).
10	Column number 8 + Column number 9.
11	Dominant path loss (column 10 vs. column 5).

Table 3.6. Description of values in variable PL_winter and PL_summer.

Variable name	Description
Streets	Results divided in areas.
Mean	Mean error for whole area.
Dest	Standard deviation for whole area.
Rms	RMS error for whole area.

Table 3.7. Description of values in variable Info_winter and Info_summer.

Street variable is a table which contains information about the 20 divided areas (see area divisions in figure 4.12). The position of the row is the number of the area, the first row is the area number 1 and the las row is the area number 20. The first, second, third and fourth column are the mean error, the standard deviation, the RMS error and the number of receiver points for every street, respectively.

Chapter 4

Results and discussions

The simulation results are analyzed and the discussions are divided into two parts: the behavior of the group of trees in different scenarios and the accuracy of the path loss obtained in comparison with summer and winter measurements.

4.1 Tree model behavior

The results obtained for the behavior of a group of tree model for different scenarios is shown in appendix D.1. Some interesting results are analyzed below.

4.1.1 Number of trees

The total number of trees depends on the diameter and separation of trees that have been selected in the scenario. It is because when the diameter of trees is larger, the distance between trees has to change accordingly, thus the density of the trees is altered too.

The number of trees obtained by the different combinations of diameter and the separation is shown in table 4.1. The examination of this table shows that the small values of diameter and the separation between trees make a high value of density of trees and on the other hand the high values of diameter and the separation show low values of density of trees.

Diam\Sep	10 m	15 m	20 m	25 m
2 m	1200	697	491	362
4 m	1125	653	471	349
6 m	1125	653	471	349
8 m	1053	619	453	337
10 m	993	584	423	318

Table 4.1. Number of trees for different combinations of diameter of the canopy and separation between trees.

4.1.2 Direct rays

Examination the number of receiver points with direct ray, as shown in figure 4.1, the lower value of diameter and high value of separation, the more direct rays.

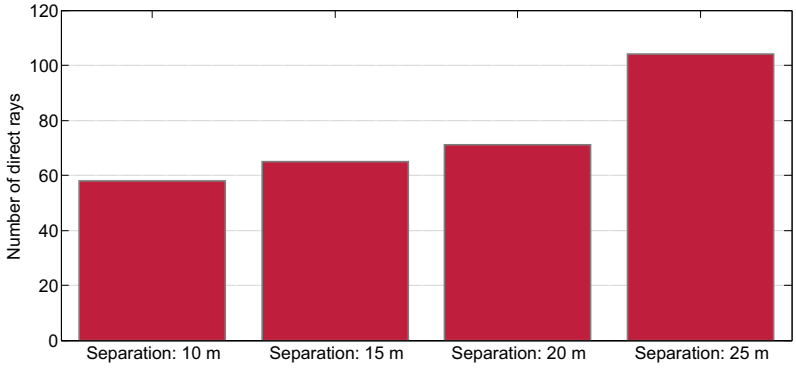

Figure 4.1. Number of direct rays. For trees of 8 faces, diameter of 6 meters and different values of separation between trees.

The number of direct rays depends on the free space between trees. Figure 4.1 shows the progression of the number of direct rays from a separation of 10 meters to a separation of 25 meters.

4.1.3 Number of no rays

The number of no ray for a scenario depends on the number of faces, the diameter of the tree and the separation between trees. In contrast to the number of direct rays, the higher value of diameter and lower value of separation between trees the more receiving points with no ray.

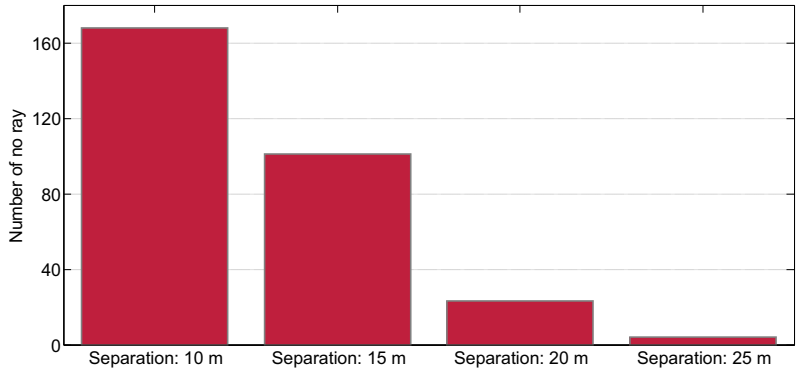

Figure 4.2. Number of no rays arriving to the receiver. For trees of 6 faces, diameter 8 meters and different values of separation between trees.

Exceptionally some times any ray is arriving to the receiver but it has been observed that as more faces the tree is modeled, the number of no rays increases with a higher value of separation. The number of no ray can be different depending on the setting of the scattering element in the ray-tracing simulator tool.

4.1.4 Mean of rays

The mean number of rays arriving at the receiver have a tendency similar to the number of direct rays, as explained in section 4.1.2.

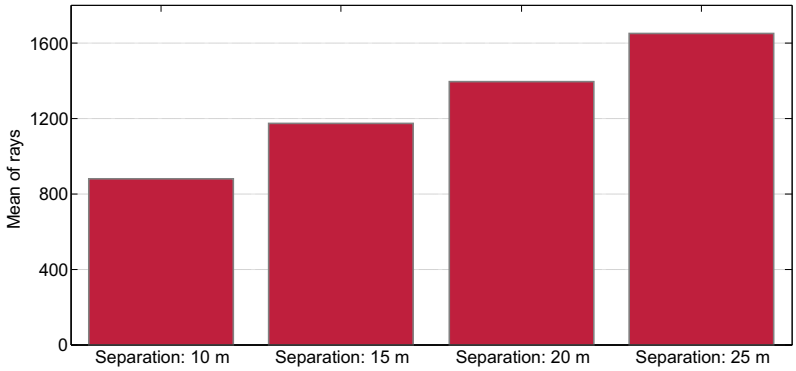

Figure 4.3. Mean of rays arriving to the receiver. For trees of 12 faces, diameter of 4 meters and different values of separation between trees.

As shown in figure 4.3 (the same tendency of figure 4.1) as more free space between trees more rays are arriving at the receiver.

4.1.5 Mean of tree rays

The number of rays reflected or scattered by a tree to the receiver vary in function of the number of faces and the diameter of the tree.

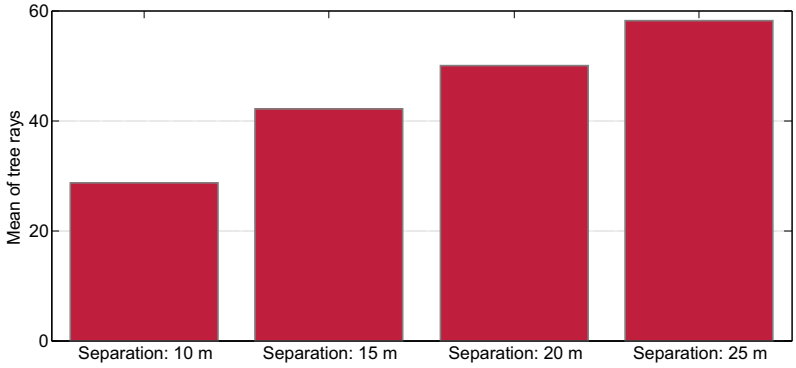

Figure 4.4. Mean of rays arriving to the receiver that are reflected or scattered by a tree . For trees of 6 faces, diameter of 10 meters and different values of separation between trees.

When a tree is modeled with a lot of faces, the area of faces is smaller and there is not ray scattered or reflected on a tree. There is a relationship

between number of faces and diameter of the tree to obtain the minimum size of side. This way, the rays will scatter or reflect on a tree. The size of the sides (L) can be obtained by,

$$L = 2r \sin\left(\frac{\pi}{n}\right) \tag{4.1}$$

Where r is the radius of the tree and n is the number of faces of the polygon. Using the equation 4.1 and the obtained information about the mean of tree rays, the minimum size of the side can be deduced to obtain a scattered or reflected ray on a tree. For $L < 2$ *meters* the tree as a scattered or reflected object is neglected by the ray tracer simulator tool.

4.1.6 Mean of tree scattered rays

The number of rays scattered by trees has the same considerations as the measurement of *mean of tree rays* (see section 4.1.5). In this case, figure 4.5 shows the percentage of rays scattered on a tree. Nearly 100 percent of rays propagated through a tree are scattered.

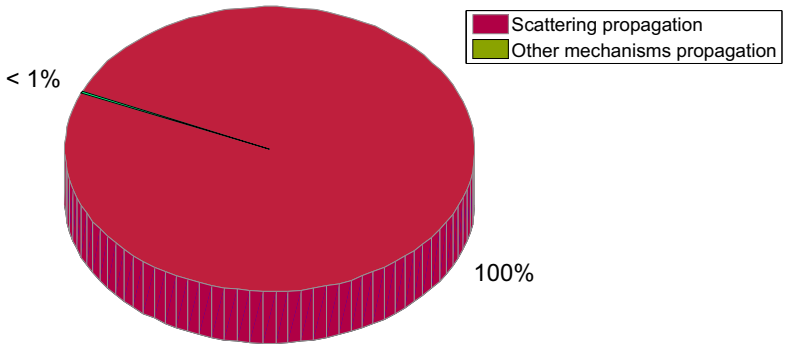

Figure 4.5. Percentage of rays scattered on a tree. For trees of 8 faces, diameter of 8 meters and separation between trees of 25 meters.

For different values of number of faces, diameter of the canopy and separation between trees, the percentage shown in figure 4.5 is always nearly 100 percent of rays are scattered.

4.2 Path Loss accuracy

The simulation results are compared with a measurement campaign conducted at Hetzwege during the summer and winter seasons. With the aim to prove the improvement of the predictions, it is compared with the results obtained for a map without vegetation.

The whole measurement data is divided into 20 groups, each group corresponds to measurements data in different street.

Measurements results

Figure 4.6 shows winter measurements and 4.7 shows summer measurements.

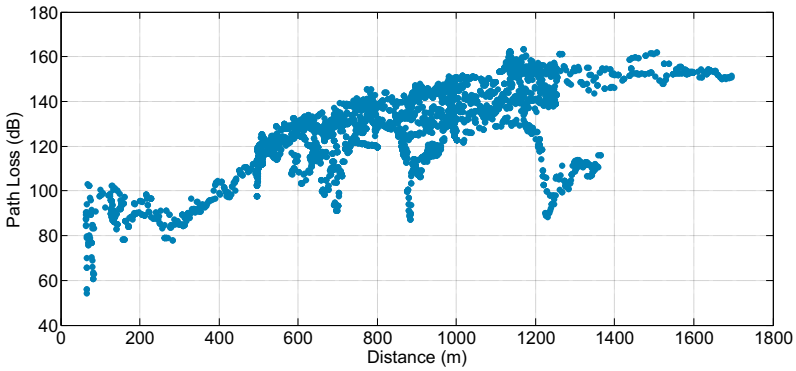

Figure 4.6. Winter measurements.

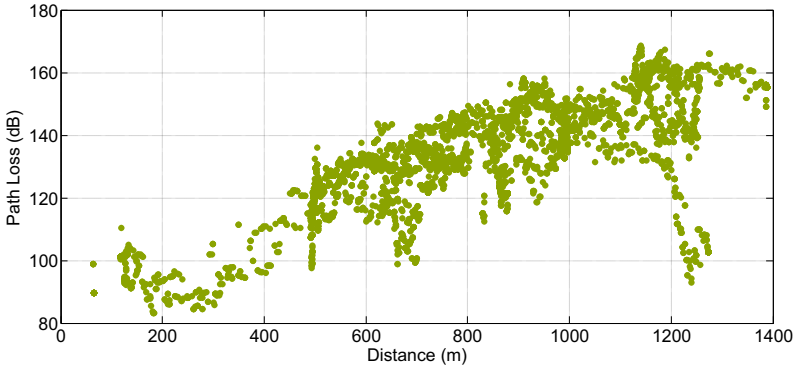

Figure 4.7. Summer measurements.

The mean path loss measured in winter is 128 dB and 133 dB in summer. The path loss measured in summer is lower than in winter. The difference of path loss between seasons can be caused by the vegetation, in summer the trees are full of leaves which are attenuating the signal received to the receiver positions in contrast to winter season where the trees are defoliated.

4.2.1 Path loss of whole area

Once the predictions results are obtained, it is compared with the measurements shown in section 4.2 (see figures 4.6 and 4.7). Figure 4.8 shows RMS error for different scenarios compared with winter and summer season predictions.

The results can be compared with a scenario without trees and for every case RMS error is higher than a scenario with trees.

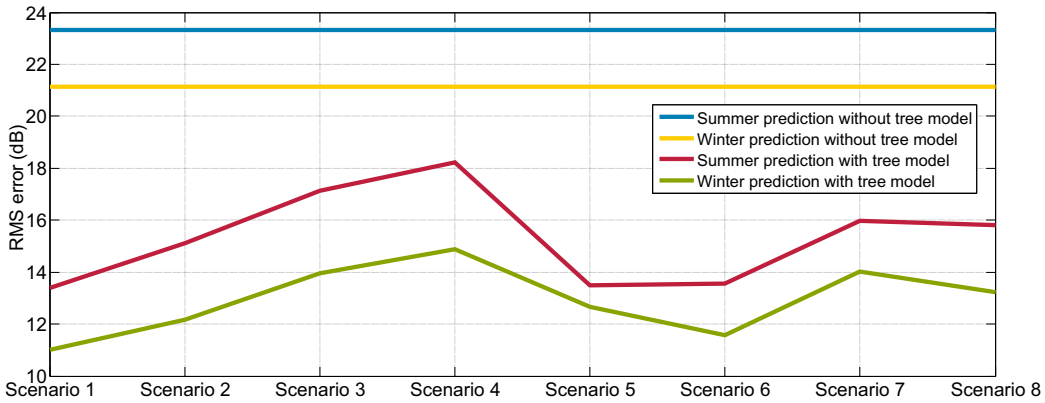

Figure 4.8. Comparison of RMS error in winter for different scenarios (see combinations of every scenario in table 3.4).

With the incorporation of the vegetation model the predictions are improved. In the best improvement, the mean error is reduced from 14.72 dB to 2.92 dB and the RMS error is reduced from 21.13 dB to 11.02 dB. The best improvement is obtained for a scenario with a group of trees modeled with polygon of 8 faces, diameter of canopy of 6 meters and separation between trees of 10 meters. More results for other scenarios are shown in table 4.2 and in appendix D.2 table II.

Scenario	Winter error		Summer error	
	Mean (dB)	RMS (dB)	Mean (dB)	RMS (dB)
Scenario 1	-2.92	11.02	-7.26	13.40
Scenario 2	-5.37	12.18	-9.77	15.10
Scenario 3	-7.68	13.97	-12.21	17.13
Scenario 4	-8.56	14.88	-13.32	18.24
Scenario 5	-1.71	12.67	-5.87	13.48
Scenario 6	-3.30	11.56	-7.29	13.56
Scenario 7	-5.36	14.02	-9.95	15.96
Scenario 8	-5.72	13.21	-10.13	15.83
Without trees	-14.73	21.14	-18.78	23.31

Table 4.2. Mean and RMS error for different scenarios (see combinations of every scenario in table 3.4).

Figure 4.8 shows winter predictions always with lower value of path loss than summer predictions, as in measurements of path loss. Also, the RMS values for predictions with tree model are in every case better than for predictions without tree model.

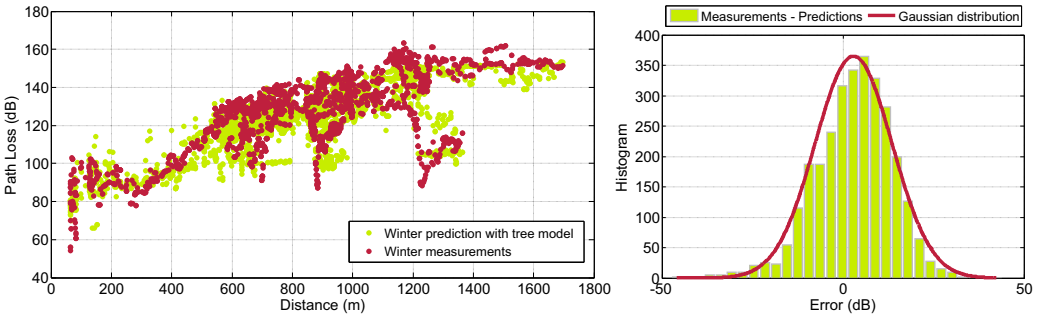

Figure 4.9. Winter prediction error with tree model.

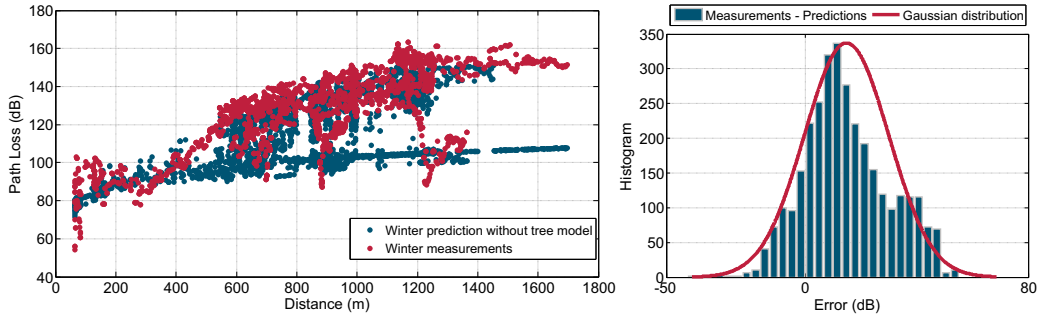

Figure 4.10. Winter prediction error without tree model.

Figures 4.9 and 4.10 show a comparison between the prediction and the measurement in winter season. Figure 4.9 takes into account a group of tree modeled with a polygon of 8 faces, diameter of 6 meters and separation between trees of 10 meters.

In case shown in figure 4.9 the mean error is 2.92 dB and the standard deviation is 10.63 dB, in contrast, the predictions without tree model, the mean error is 14.72 dB and the standard deviation is 15.16 dB.

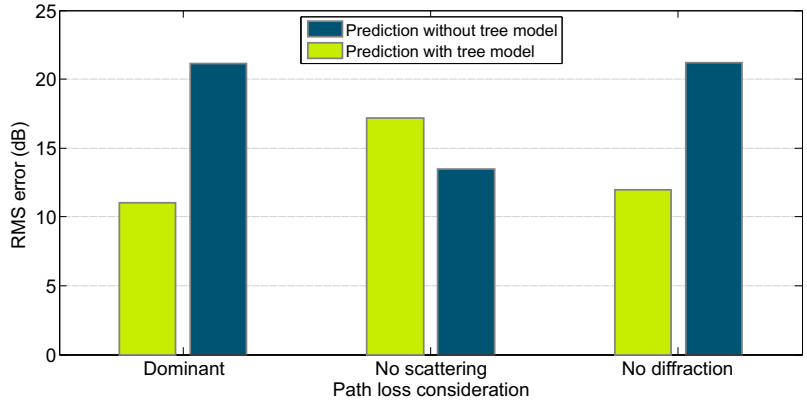

Figure 4.11. RMS error in winter. Scattering vs. Diffraction.

The importance of tree scattering can be shown in figure 4.11. When the mechanism dominant is considered, a prediction with tree model has more accurate results but if the scattering is not considered, RMS error changes and a prediction without tree model has more accurate results. Furthermore, if diffraction is not considered, RMS error of a prediction with tree model

has more accurate results.

Figure 4.11 is calculated for a group of trees modeled with a polygon of 8 faces, diameter of canopy of 6 meters and separation between trees of 10 meters. More results for different scenarios in appendix D.2

As shows figure 4.5, nearly 100 percent of rays propagated through a tree are scattered, also, as shows figure 4.11, the most part of the prediction loss appears to be dominated by the fields scattered on the trees. This interpretation agrees with previous works about propagation loss through vegetation [9].

4.2.2 Path loss of every street

With the aim to analyze the predictions in different areas, the receiver positions are divided into 20 groups, each group corresponds to measurements data in different street. Figure 4.12 shows the division areas where some areas are not shadowed by trees and others areas are covered by trees.

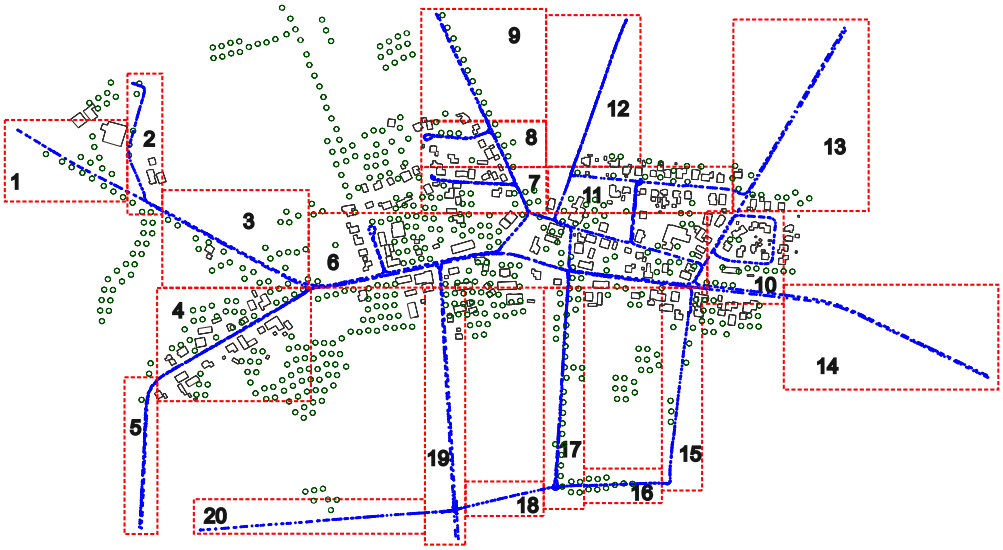

Figure 4.12. Receiver points.

Tables V and VI from appendix D.3 show the RMS error results divided into the 20 different areas and compared with different scenarios and predic-

tion without trees. In tables VII and VIII there are the number of receiver position used to calculate RMS error for every street and tables IV up to XI show mean error and standard deviation for winter and summer season.

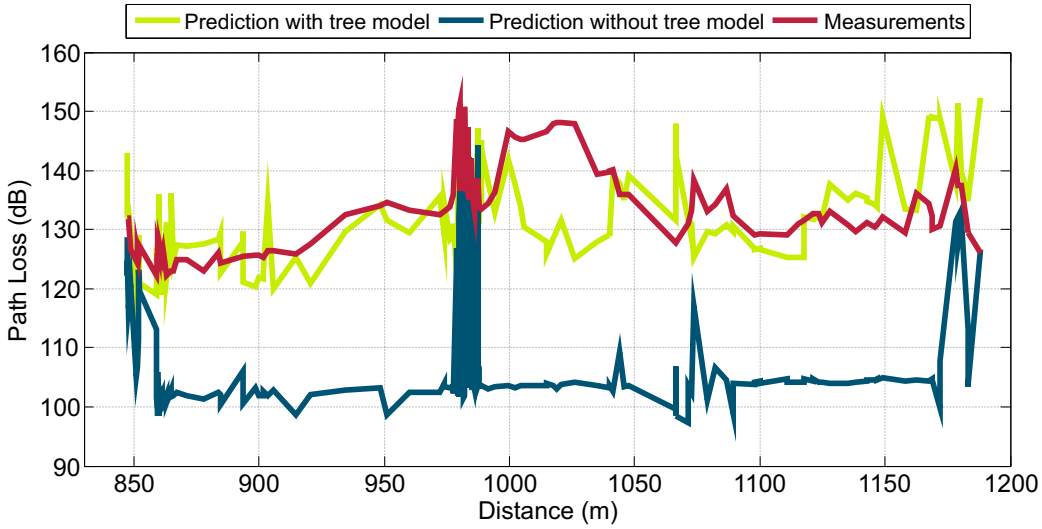

Figure 4.13. Comparison of path loss prediction for winter season in area number 11.

Figure 4.13 shows a comparison of path loss in area number 11 of the map in winter season. Prediction with tree model has an accuracy RMS error of 9.83 dB and prediction without tree model of 25.93 dB. Tree model used is a polygon of 8 faces, diameter of canopy of 6 meters and separation between trees of 10 meters. The prediction with tree model is most of the time following the values of measurement.

Before obtain results for different areas, the path loss prediction was expected to be accurate in areas which are not shadowed by trees because the coherent field is not considered in this thesis and it was assume to be the responsible of the accuracy in receiver points situated in areas covered by trees.

After to analyze the results, the coherent field doesn't give the idea to be the parameter responsible of not accurate results in some areas covered by trees, but as shows figure 4.14, for whole area, the path loss prediction gives the impression to be accurate at large distances from the base station where

the multiple scattering propagation mode (incoherent field) is dominate [28].

Figure 4.14. Error for every receiver point divided into three groups.

As can be seen in figure 4.14 the most of the highest values of error are near the base station (on the left upper corner of the figure) and around the vegetation (center of the figure). The accurate predictions are on the right lower corner of the figure where there are not trees and the receiver points are at large distance from the base station.

Chapter 5

Conclusions

In this thesis, a tree model and a group of trees model have been designed and created with the aim to derive the incoherent scattering field on a tree and to improve the prediction of path loss in rural areas. The scattered fields on trees reported from previous works [12, 13, 17, 18] have been used with adaptation to the ray tracing simulation. The simulations have been divided into two groups. In the first one is analyzed the behavior of the group of trees in different scenarios and in the second one is analyzed the accuracy of the path loss. The predictions were compared with a measurement campaign conducted at Hetzwege, Germany, during the summer and winter season, where a WiMAX system operating at 3.5 GHz provides broadband wireless access to the village.

The group of trees model is defined by the parameters: number of faces of the polygon, diameter of the canopy and separation between trees.

It was observed that the number of the reays increases when the group of trees is modeled with large separation between trees in comparison with the diameter of the canopy and nearly 100 percent of the rays propagated on a tree were scattered.

With the incorporation of the vegetation model created, the prediction in a rural area is improved. The mean error is reduced from 14.72 dB to 2.92 dB and the RMS error is reduced from 21.13 dB to 11.02 dB. The best improvement was obtained with a group of trees modeled with a polygon of

8 faces, diameter of canopy of 6 meters and separation between trees of 10 meters.

The predictions in summer season have higher values of path loss in comparison with winter season, as the measurement results.

The scattered rays propagated on a tree have been demonstrated to be an important field to take into account.

The predictions give the impression to be accurate when are at large distances from the base station and from the vegetation. This effect can be explained as the result of the interplay between the direct path propagation mode (coherent field) and the multiple scattering propagation mode (incoherent field) [28].

A tree is hard to model due to the fact that the composition of a tree is complex and it is different during the season changes. For radio network planner in rural areas, the inclusion of a vegetation model is important to improve the path loss prediction hence In this thesis with the vegetation model designed the path loss has been improved satisfactorily.

Appendices

Appendix A

Flowchart Functions

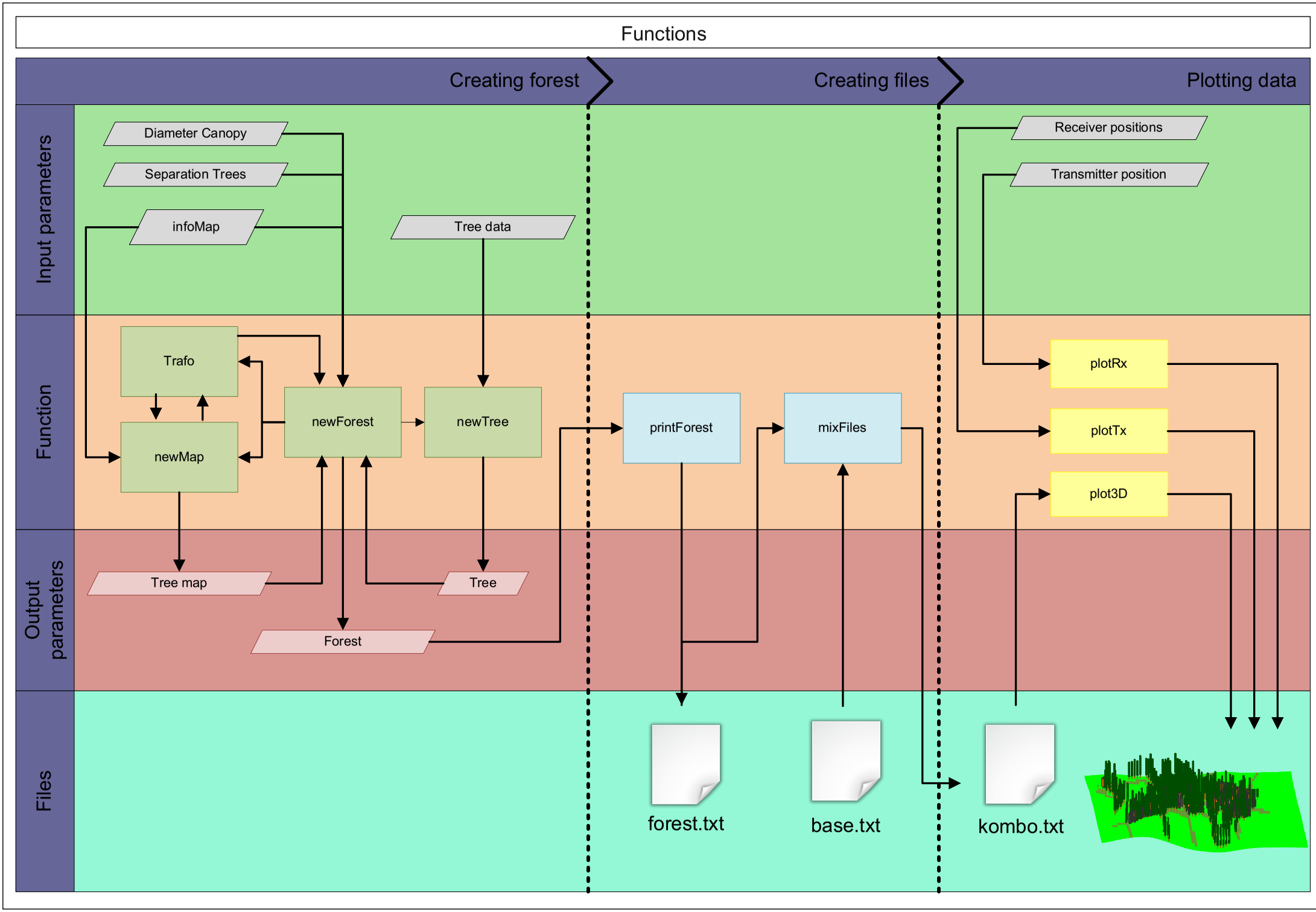
Functions
Creating forest
Creating files
Plotting data
Input parameters
Function
Output parameters
Files
Diameter Canopy
Separation Trees
infoMap
Tree data
Receiver positions
Transmitter position
Trafo
newMap
newForest
newTree
printForest
mixFiles
plotRx
plotTx
plot3D
Tree map
Tree
Forest
forest.txt
base.txt
kombo.txt

Appendix B

Forest Structure

Forest class

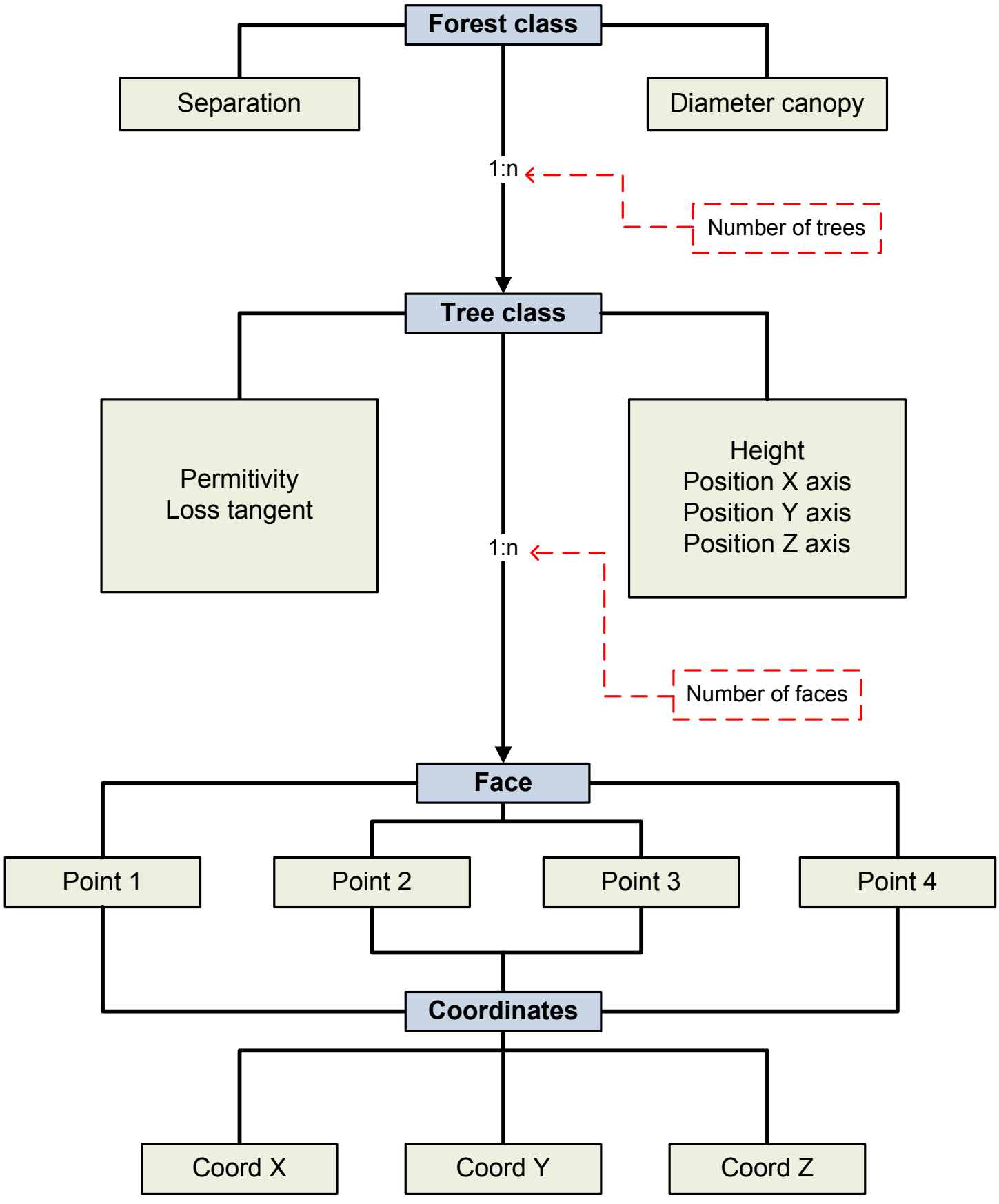

Appendix C

Top view forest maps

a) Diameter canopy = 4m | Separation = 10m

b) Diameter canopy = 4m | Separation = 15m

c) Diameter canopy = 4m | Separation = 20m

d) Diameter canopy = 4m | Separation = 25m

e) Diameter canopy = 6m | Separation = 10m

f) Diameter canopy = 6m | Separation = 15m

g) Diameter canopy = 6m | Separation = 20m

h) Diameter canopy = 6m | Separation = 25m

i) Diameter canopy = 10m | Separation = 10m

j) Diameter canopy = 10m | Separation = 15m

k) Diameter canopy = 10m | Separation = 20m

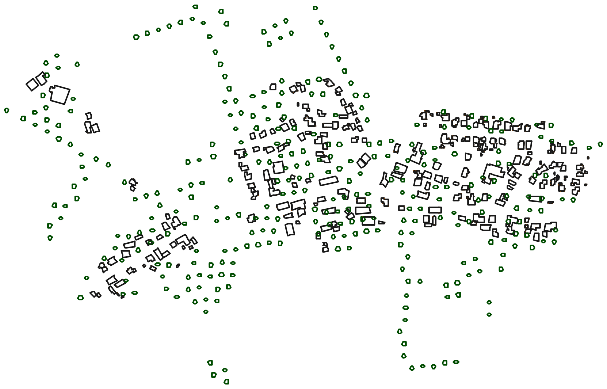

l) Diameter canopy = 10m | Separation = 25m

Appendix D

Results

D.1 Tables. Tree model behavior

Table I: Tree model behavior (1 of 2)

Scenario	Faces	Diameter (m)	Separation (m)	Trees	Direct ray	No ray	Mean of rays	Mean of tree rays	Mean of tree scattered rays
1	6	2	10	1200	96	11	1340,21	0,03	0,00
2	6	2	15	697	125	3	1735,16	0,04	0,00
3	6	2	20	491	135	0	1998,59	0,03	0,00
4	6	2	25	362	146	0	2154,04	0,02	0,00
5	6	4	10	1125	74	3	969,45	55,52	55,49
6	6	4	15	653	93	0	1292,58	77,71	77,68
7	6	4	20	471	105	0	1515,58	79,84	79,81
8	6	4	25	349	127	1	1772,70	79,49	79,45
9	6	6	10	1125	59	15	735,35	62,59	62,58
10	6	6	15	653	68	1	1007,32	89,47	89,44
11	6	6	20	471	75	0	1176,99	96,10	96,08
12	6	6	25	349	107	1	1440,08	104,72	104,70
13	6	8	10	1053	47	28	531,35	36,70	36,69
14	6	8	15	619	67	8	811,86	54,34	54,32
15	6	8	20	453	64	0	933,85	62,33	62,31
16	6	8	25	337	90	1	1179,50	73,26	73,22
17	6	10	10	993	47	20	479,73	28,66	28,64
18	6	10	15	584	59	8	727,30	42,06	42,04
19	6	10	20	423	51	0	795,30	49,93	49,91
20	6	10	25	318	86	1	1040,47	58,25	58,23
21	8	2	10	1200	96	11	1305,23	0,07	0,00
22	8	2	15	697	123	3	1695,24	0,04	0,00
23	8	2	20	491	134	0	1971,04	0,05	0,00
24	8	2	25	362	142	0	2135,57	0,06	0,00
25	8	4	10	1125	72	108	880,97	0,05	0,00
26	8	4	15	653	91	4	1176,87	0,05	0,00
27	8	4	20	471	103	0	1399,16	0,04	0,00
28	8	4	25	349	124	1	1655,34	0,05	0,00
29	8	6	10	1125	58	13	708,64	65,47	65,43
30	8	6	15	653	65	0	991,23	103,05	103,02
31	8	6	20	471	71	0	1164,77	119,81	119,77
32	8	6	25	349	104	1	1423,97	127,01	126,96
33	8	8	10	1053	47	24	508,42	39,62	39,59
34	8	8	15	619	63	5	779,59	58,61	58,59
35	8	8	20	453	64	0	899,09	75,32	75,31
36	8	8	25	337	86	1	1150,48	84,78	84,70
37	8	10	10	993	47	26	458,58	27,98	27,97
38	8	10	15	584	56	8	690,95	43,27	43,25
39	8	10	20	423	49	0	768,19	56,52	56,48
40	8	10	25	318	86	1	1005,34	68,82	68,79

Table I: Tree model behavior (2 of 2)

Scenario	Faces	Diameter (m)	Separation (m)	Trees	Direct ray	No ray	Mean of rays	Mean of tree rays	Mean of tree scattered rays
41	12	2	10	1200	96	11	1299,73	0,02	0,00
42	12	2	15	697	123	3	1690,25	0,04	0,00
43	12	2	20	491	134	0	1965,97	0,04	0,00
44	12	2	25	362	142	0	2131,36	0,05	0,00
45	12	4	10	1125	72	107	877,82	0,03	0,00
46	12	4	15	653	91	4	1171,49	0,07	0,00
47	12	4	20	471	103	0	1392,36	0,06	0,00
48	12	4	25	349	124	1	1650,31	0,08	0,00
49	12	6	10	1125	58	157	640,11	0,03	0,00
50	12	6	15	653	65	51	883,45	0,06	0,00
51	12	6	20	471	71	13	1037,75	0,06	0,00
52	12	6	25	349	103	1	1290,41	0,07	0,00
53	12	8	10	1053	47	14	522,72	58,85	58,84
54	12	8	15	619	63	5	808,43	92,60	92,59
55	12	8	20	453	63	0	931,22	112,28	112,25
56	12	8	25	337	86	1	1185,55	127,47	127,42
57	12	10	10	993	47	24	469,67	41,82	41,81
58	12	10	15	584	56	6	709,74	65,91	65,90
59	12	10	20	423	49	0	790,67	86,27	86,25
60	12	10	25	318	86	1	1034,54	103,50	103,47
61	16	2	10	1200	96	11	1295,50	0,04	0,00
62	16	2	15	697	123	3	1687,51	0,12	0,00
63	16	2	20	491	134	0	1963,95	0,05	0,00
64	16	2	25	362	142	0	2129,05	0,07	0,00
65	16	4	10	1125	72	108	874,90	0,03	0,00
66	16	4	15	653	91	11	1169,46	0,05	0,00
67	16	4	20	471	103	0	1389,26	0,04	0,00
68	16	4	25	349	124	1	1647,45	0,06	0,00
69	16	6	10	1125	58	157	638,63	0,03	0,00
70	16	6	15	653	65	51	881,97	0,03	0,00
71	16	6	20	471	71	15	1034,47	0,04	0,00
72	16	6	25	349	104	1	1287,99	0,09	0,00
73	16	8	10	1053	45	168	461,36	0,02	0,00
74	16	8	15	619	62	101	713,98	0,02	0,00
75	16	8	20	453	64	23	816,15	0,04	0,00
76	16	8	25	337	85	4	1054,71	0,06	0,00
77	16	10	10	993	47	26	458,58	27,98	27,97
78	16	10	15	584	56	112	642,46	0,03	0,00
79	16	10	20	423	49	33	702,12	0,05	0,00
80	16	10	25	318	86	22	929,01	0,07	0,00

D.2 Tables. Path loss accuracy whole area

Table II: Prediction error

				Winter predictions			Summer predictions		
Scenario	Faces	Diameter (m)	Separation (m)	Mean error (dB)	Standard deviation (dB)	RMS error (dB)	Mean error (dB)	Standard deviation (dB)	RMS error (dB)
1	8	6	10	-2,92	10,63	11,02	-7,26	11,26	13,40
2	8	6	15	-5,37	10,93	12,18	-9,77	11,52	15,10
3	8	6	20	-7,68	11,68	13,97	-12,21	12,01	17,13
4	8	6	25	-8,56	12,17	14,88	-13,32	12,46	18,24
5	8	10	10	-1,71	12,56	12,67	-5,87	12,14	13,48
6	8	10	15	-3,30	11,08	11,56	-7,29	11,44	13,56
7	8	10	20	-5,36	12,96	14,02	-9,95	12,48	15,96
8	8	10	25	-5,72	11,91	13,21	-10,13	12,16	15,83
			No trees	-14,73	15,16	21,14	-18,78	13,80	23,31

Table III: Prediction error (no scattering)

				Winter predictions			Summer predictions		
Scenario	Faces	Diameter (m)	Separation (m)	Mean error (dB)	Standard deviation (dB)	RMS error (dB)	Mean error (dB)	Standard deviation (dB)	RMS error (dB)
1	8	6	10	9,82	14,10	17,18	3,97	13,55	14,11
2	8	6	15	8,54	14,27	16,63	3,00	13,93	14,25
3	8	6	20	8,51	14,25	16,59	2,84	13,90	14,19
4	8	6	25	8,47	14,25	16,57	2,83	13,90	14,18
5	8	10	10	10,10	14,71	17,84	4,77	14,22	14,99
6	8	10	15	9,13	14,42	17,06	3,72	13,91	14,39
7	8	10	20	8,58	14,28	16,66	2,97	13,97	14,28
8	8	10	25	8,73	14,28	16,73	3,00	13,92	14,24
			No trees	4,62	12,66	13,48	-1,56	13,32	13,41

Table IV: Prediction error (no diffraction)

				Winter predictions			Summer predictions		
Scenario	Faces	Diameter (m)	Separation (m)	Mean error (dB)	Standard deviation (dB)	RMS error (dB)	Mean error (dB)	Standard deviation (dB)	RMS error (dB)
1	8	6	10	-1,52	11,89	11,99	-5,52	12,60	13,76
2	8	6	15	-4,54	11,72	12,57	-8,64	12,34	15,07
3	8	6	20	-7,19	12,19	14,16	-11,72	12,49	17,13
4	8	6	25	-8,20	12,65	15,07	-12,92	12,92	18,27
5	8	10	10	0,12	14,49	14,49	-3,76	14,27	14,75
6	8	10	15	-1,81	12,37	12,50	-5,64	12,67	13,87
7	8	10	20	-4,64	13,66	14,43	-9,10	13,27	16,09
8	8	10	25	-4,68	13,12	13,93	-8,90	13,65	16,29
			No trees	-14,03	15,90	21,20	-18,02	14,16	22,92

D.3 Tables. Path loss accuracy divided area

Table V: RMS error in winter season (dB)

Area	Faces: 8. Diameter: 6 m. Separation: 10 m.	Faces: 8. Diameter: 6 m. Separation: 15 m.	Faces: 8. Diameter: 6 m. Separation: 20 m.	Faces: 8. Diameter: 6 m. Separation: 25 m.	Faces: 8. Diameter: 10 m. Separation: 10 m.	Faces: 8. Diameter: 10 m. Separation: 15 m.	Faces: 8. Diameter: 10 m. Separation: 20 m.	Faces: 8. Diameter: 10 m. Separation: 25 m.	No trees
Num. 1	5,32	6,61	6,72	6,81	9,40	7,91	6,04	5,86	7,12
Num. 2	13,50	13,01	12,00	12,31	14,44	12,79	13,41	13,44	13,26
Num. 3	8,36	8,13	8,77	8,21	9,43	7,62	7,69	7,71	9,67
Num. 4	0,28	0,04	0,07	7,69	8,82	2,43	2,98	4,04	20,26
Num. 5	16,89	17,21	18,10	20,67	15,59	16,65	18,00	19,34	26,30
Num. 6	12,65	14,18	16,10	18,32	14,54	14,04	17,36	15,94	21,73
Num. 7	8,42	7,81	9,80	9,92	11,50	8,95	10,01	7,51	12,48
Num. 8	13,81	11,71	12,09	12,76	13,90	14,37	15,85	15,95	13,00
Num. 9	8,51	12,03	11,74	11,58	10,79	8,03	11,06	10,89	14,89
Num. 10	7,38	8,75	12,81	17,47	8,95	8,51	10,18	11,94	19,10
Num. 11	9,83	9,72	11,22	13,14	11,18	11,01	11,14	12,02	25,93
Num. 12	13,32	14,21	15,73	13,91	16,77	14,77	16,17	13,16	14,25
Num. 13	16,39	16,51	16,69	13,68	21,63	17,00	21,48	16,71	11,25
Num. 14	6,56	10,11	15,51	14,27	4,94	4,53	8,10	12,86	37,48
Num. 15	8,30	15,32	19,89	21,13	7,28	9,52	11,69	18,42	21,34
Num. 16	7,96	11,23	15,12	14,24	11,79	5,68	14,17	12,11	36,67
Num. 17	9,16	13,08	13,63	14,68	4,17	6,83	16,06	10,27	30,11
Num. 18	6,59	5,17	3,13	3,39	7,55	5,58	5,39	4,21	7,78
Num. 19	8,78	8,45	10,12	12,11	7,69	6,69	9,76	8,56	16,57
Num. 20	NaN	NaN	NaN	NaN	NaN	NaN	NaN	NaN	NaN

Table VI: RMS error in summer season (dB)

Area	Faces: 8. Diameter: 6 m. Separation: 10 m.	Faces: 8. Diameter: 6 m. Separation: 15 m.	Faces: 8. Diameter: 6 m. Separation: 20 m.	Faces: 8. Diameter: 6 m. Separation: 25 m.	Faces: 8. Diameter: 10 m. Separation: 10 m.	Faces: 8. Diameter: 10 m. Separation: 15 m.	Faces: 8. Diameter: 10 m. Separation: 20 m.	Faces: 8. Diameter: 10 m. Separation: 25 m.	No trees
Num. 1	9,36	9,96	10,55	10,53	9,78	10,53	10,19	9,58	11,07
Num. 2	19,10	11,66	11,11	8,99	10,55	10,53	10,15	10,21	15,76
Num. 3	9,38	10,93	11,56	11,21	9,60	11,06	11,13	11,21	12,84
Num. 4	9,44	11,07	13,18	13,17	7,72	9,82	10,40	11,62	18,21
Num. 5	26,07	26,36	25,84	26,47	25,26	25,89	25,82	25,81	34,26
Num. 6	14,37	16,66	18,96	20,90	15,42	15,56	19,25	18,40	24,63
Num. 7	11,65	11,25	12,77	12,49	13,47	12,05	13,66	10,44	14,94
Num. 8	8,69	8,37	14,44	10,11	9,26	8,88	10,14	10,46	16,04
Num. 9	9,81	12,47	13,47	13,74	11,17	10,28	11,95	12,83	16,89
Num. 10	9,51	11,06	14,95	16,58	8,49	9,51	11,47	12,23	17,70
Num. 11	8,71	8,20	9,11	10,70	10,11	8,94	9,59	10,31	26,93
Num. 12	5,21	6,01	5,74	8,41	9,02	7,69	5,54	5,21	10,08
Num. 13	20,44	20,58	20,67	18,32	24,92	21,80	25,87	19,66	10,14
Num. 14	10,67	15,02	22,01	20,09	9,80	9,82	12,86	15,52	12,53
Num. 15	10,64	17,00	21,23	23,55	8,56	11,96	14,32	18,82	25,18
Num. 16	5,09	11,12	18,51	19,08	NaN	4,20	16,78	13,52	40,14
Num. 17	14,35	19,20	20,97	23,72	5,99	10,34	18,15	18,78	31,82
Num. 18	NaN	NaN	NaN	NaN	NaN	NaN	NaN	NaN	NaN
Num. 19	10,45	10,58	13,30	15,37	9,31	11,01	11,88	10,93	16,97
Num. 20	NaN	NaN	NaN	NaN	NaN	NaN	NaN	NaN	NaN

Table VII: Number of receiver points in winter season

Area	Faces: 8. Diameter: 6 m. Separation: 10 m.	Faces: 8. Diameter: 6 m. Separation: 15 m.	Faces: 8. Diameter: 6 m. Separation: 20 m.	Faces: 8. Diameter: 6 m. Separation: 25 m.	Faces: 8. Diameter: 10 m. Separation: 10 m.	Faces: 8. Diameter: 10 m. Separation: 15 m.	Faces: 8. Diameter: 10 m. Separation: 20 m.	Faces: 8. Diameter: 10 m. Separation: 25 m.	No trees
Num. 1	52	52	52	52	52	52	52	52	52
Num. 2	77	80	81	81	81	81	81	81	81
Num. 3	151	151	151	151	151	151	151	151	151
Num. 4	1	1	1	1	1	1	1	1	1
Num. 5	43	43	43	43	43	43	43	43	43
Num. 6	683	722	730	732	552	676	724	716	732
Num. 7	223	224	224	224	219	224	224	224	224
Num. 8	151	151	151	151	151	151	151	151	151
Num. 9	88	88	88	88	88	88	88	88	88
Num. 10	113	152	155	163	82	116	143	125	163
Num. 11	249	249	249	249	246	249	249	249	249
Num. 12	264	264	264	264	264	264	264	264	264
Num. 13	122	122	122	122	122	122	122	122	122
Num. 14	166	166	166	166	163	166	166	166	166
Num. 15	120	141	141	141	69	110	141	141	141
Num. 16	13	76	78	78	1	39	68	76	80
Num. 17	163	185	189	189	127	157	187	187	189
Num. 18	35	35	35	35	35	35	35	35	35
Num. 19	163	163	163	163	163	163	163	163	163
Num. 20	0	0	0	0	0	0	0	0	0

Table VIII: Number of receiver points in summer season

Area	Faces: 8. Diameter: 6 m. Separation: 10 m.	Faces: 8. Diameter: 6 m. Separation: 15 m.	Faces: 8. Diameter: 6 m. Separation: 20 m.	Faces: 8. Diameter: 6 m. Separation: 25 m.	Faces: 8. Diameter: 10 m. Separation: 10 m.	Faces: 8. Diameter: 10 m. Separation: 15 m.	Faces: 8. Diameter: 10 m. Separation: 20 m.	Faces: 8. Diameter: 10 m. Separation: 25 m.	No trees
Num. 1	51	51	51	51	51	51	51	51	51
Num. 2	18	20	20	20	20	20	20	20	20
Num. 3	164	164	164	164	164	164	164	164	164
Num. 4	148	148	148	148	148	148	148	148	148
Num. 5	152	152	152	152	152	152	152	152	152
Num. 6	626	649	668	673	526	622	644	661	673
Num. 7	182	183	183	183	176	183	183	183	183
Num. 8	111	111	111	111	111	111	111	111	111
Num. 9	87	87	87	87	87	87	87	87	87
Num. 10	108	118	121	121	74	93	116	105	121
Num. 11	245	245	245	245	242	245	245	245	245
Num. 12	45	45	45	45	45	45	45	45	45
Num. 13	71	71	71	71	71	71	71	71	71
Num. 14	25	25	25	25	23	25	25	25	25
Num. 15	137	177	178	178	64	128	178	178	178
Num. 16	9	48	49	49	0	30	40	49	49
Num. 17	253	276	290	290	186	245	280	288	290
Num. 18	0	0	0	0	0	0	0	0	0
Num. 19	148	148	148	148	148	148	148	148	148
Num. 20	0	0	0	0	0	0	0	0	0

Table IX: Mean error in winter season (Measurement - Prediction)

Area	Faces: 8. Diameter: 6 m. Separation: 10 m.	Faces: 8. Diameter: 6 m. Separation: 15 m.	Faces: 8. Diameter: 6 m. Separation: 20 m.	Faces: 8. Diameter: 6 m. Separation: 25 m.	Faces: 8. Diameter: 10 m. Separation: 10 m.	Faces: 8. Diameter: 10 m. Separation: 15 m.	Faces: 8. Diameter: 10 m. Separation: 20 m.	Faces: 8. Diameter: 10 m. Separation: 25 m.	No trees
Num. 1	0,14	0,06	1,59	0,96	3,05	0,00	1,96	0,98	3,62
Num. 2	1,15	0,79	0,96	0,89	1,35	0,05	0,68	0,54	4,48
Num. 3	0,36	0,64	1,42	1,35	2,51	0,96	1,65	1,68	2,11
Num. 4	0,28	0,04	0,07	7,69	8,82	2,43	2,98	4,04	20,26
Num. 5	15,21	15,51	16,87	19,13	13,93	15,17	16,81	18,51	26,13
Num. 6	9,37	12,29	14,50	16,12	11,88	11,42	14,39	14,12	18,32
Num. 7	6,54	5,84	7,49	8,27	10,34	7,30	8,70	6,34	8,90
Num. 8	9,84	7,42	0,74	7,40	9,60	10,32	12,12	12,04	3,60
Num. 9	4,37	6,04	4,38	4,83	0,01	2,39	2,10	3,10	12,61
Num. 10	1,15	5,86	9,56	12,13	0,24	6,01	7,40	5,11	14,12
Num. 11	3,53	3,53	5,65	7,26	3,01	3,03	2,82	4,11	23,62
Num. 12	0,63	1,99	1,38	2,26	9,87	2,97	4,05	0,39	10,10
Num. 13	9,61	8,16	7,57	3,60	14,41	10,51	12,66	7,09	4,50
Num. 14	4,55	8,53	14,02	12,65	3,12	2,12	6,70	11,17	31,24
Num. 15	4,32	12,07	17,09	19,50	2,49	4,93	9,20	15,99	16,08
Num. 16	3,43	2,44	10,32	12,14	11,79	4,93	9,98	8,36	36,57
Num. 17	1,82	11,12	8,61	11,38	0,57	2,05	12,70	4,44	26,46
Num. 18	5,79	4,71	0,83	1,79	7,12	4,57	2,77	1,93	7,35
Num. 19	0,92	1,68	2,69	4,07	1,30	1,57	0,08	0,07	2,41
Num. 20	NaN	NaN	NaN	NaN	NaN	NaN	NaN	NaN	NaN

Table X: Mean error in summer season (Measurement - Prediction)

Area	Faces: 8. Diameter: 6 m. Separation: 10 m.	Faces: 8. Diameter: 6 m. Separation: 15 m.	Faces: 8. Diameter: 6 m. Separation: 20 m.	Faces: 8. Diameter: 6 m. Separation: 25 m.	Faces: 8. Diameter: 10 m. Separation: 10 m.	Faces: 8. Diameter: 10 m. Separation: 15 m.	Faces: 8. Diameter: 10 m. Separation: 20 m.	Faces: 8. Diameter: 10 m. Separation: 25 m.	No trees
Num. 1	3,84	5,60	2,62	7,45	0,56	3,60	6,84	5,71	9,70
Num. 2	8,31	6,53	3,24	3,36	4,54	3,96	7,59	6,37	14,49
Num. 3	3,22	4,35	5,31	5,01	1,26	4,79	5,38	5,37	5,78
Num. 4	1,81	3,24	8,75	9,51	2,14	0,35	3,60	5,35	15,37
Num. 5	25,40	25,70	25,12	25,74	24,44	25,29	25,18	25,23	34,01
Num. 6	11,77	14,84	16,99	18,60	13,28	13,22	17,08	16,30	21,70
Num. 7	9,42	9,23	10,52	10,86	12,69	10,86	12,17	9,38	11,76
Num. 8	4,02	0,74	10,96	1,48	6,98	5,79	5,01	4,41	13,59
Num. 9	7,90	8,58	8,45	9,63	1,54	4,54	7,06	7,83	15,54
Num. 10	3,35	7,71	11,22	10,41	0,49	6,96	8,41	4,44	13,46
Num. 11	2,58	2,51	4,40	5,91	1,83	2,05	1,96	2,60	24,58
Num. 12	0,04	1,25	1,14	3,27	8,09	1,93	1,56	2,05	4,62
Num. 13	16,34	16,89	14,93	9,16	21,37	17,71	21,51	13,26	3,55
Num. 14	10,54	14,60	21,57	19,79	9,59	9,63	12,66	14,73	12,00
Num. 15	4,68	13,29	17,29	21,44	1,82	5,39	10,86	16,42	21,04
Num. 16	4,88	2,30	13,70	16,15	NaN	3,72	10,73	9,97	40,09
Num. 17	10,60	17,65	18,31	21,71	4,76	6,91	15,29	14,70	28,09
Num. 18	NaN	NaN	NaN	NaN	NaN	NaN	NaN	NaN	NaN
Num. 19	7,51	7,15	10,06	11,82	7,34	10,05	8,89	8,29	10,84
Num. 20	NaN	NaN	NaN	NaN	NaN	NaN	NaN	NaN	NaN

Table XI: Standard deviation in winter season

Area	Faces: 8. Diameter: 6 m. Separation: 10 m.	Faces: 8. Diameter: 6 m. Separation: 15 m.	Faces: 8. Diameter: 6 m. Separation: 20 m.	Faces: 8. Diameter: 6 m. Separation: 25 m.	Faces: 8. Diameter: 10 m. Separation: 10 m.	Faces: 8. Diameter: 10 m. Separation: 15 m.	Faces: 8. Diameter: 10 m. Separation: 20 m.	Faces: 8. Diameter: 10 m. Separation: 25 m.	No trees
Num. 1	5,37	6,68	6,59	6,80	8,98	7,99	5,77	5,83	6,19
Num. 2	13,54	13,07	12,04	12,35	14,47	12,87	13,48	13,51	12,56
Num. 3	8,38	8,13	8,68	8,13	9,12	7,58	7,54	7,54	9,46
Num. 4	0,00	0,00	0,00	0,00	0,00	0,00	0,00	0,00	0,00
Num. 5	7,43	7,55	6,64	7,92	7,08	6,93	6,52	5,70	3,03
Num. 6	8,51	7,09	7,00	8,72	8,40	8,18	9,72	7,40	11,68
Num. 7	5,32	5,20	6,34	5,48	5,04	5,20	4,95	4,02	8,76
Num. 8	9,73	9,09	12,11	10,43	10,09	10,04	10,24	10,49	12,53
Num. 9	7,35	10,46	10,95	10,58	10,85	7,71	10,92	10,50	7,97
Num. 10	7,33	6,52	8,55	12,61	9,00	6,06	7,02	10,83	12,90
Num. 11	9,19	9,07	9,71	10,97	10,79	10,60	10,80	11,31	10,71
Num. 12	13,33	14,09	15,70	13,75	13,59	14,50	15,69	13,18	10,07
Num. 13	13,33	14,41	14,94	13,25	16,20	13,43	17,42	15,19	10,35
Num. 14	4,75	5,44	6,66	6,62	3,85	4,01	4,56	6,40	20,78
Num. 15	7,11	9,46	10,21	8,17	6,89	8,18	7,25	9,17	14,08
Num. 16	7,47	11,03	11,13	7,49	0,00	2,85	10,14	8,82	2,67
Num. 17	9,01	6,92	10,60	9,29	4,15	6,53	9,85	9,28	14,40
Num. 18	3,18	2,17	3,06	2,92	2,56	3,25	4,69	3,79	2,59
Num. 19	8,76	8,31	9,78	11,44	7,60	6,53	9,79	8,59	16,45
Num. 20	NaN	NaN	NaN	NaN	NaN	NaN	NaN	NaN	NaN

Table XII: Standard deviation in summer season

Area	Faces: 8. Diameter: 6 m. Separation: 10 m.	Faces: 8. Diameter: 6 m. Separation: 15 m.	Faces: 8. Diameter: 6 m. Separation: 20 m.	Faces: 8. Diameter: 6 m. Separation: 25 m.	Faces: 8. Diameter: 10 m. Separation: 10 m.	Faces: 8. Diameter: 10 m. Separation: 15 m.	Faces: 8. Diameter: 10 m. Separation: 20 m.	Faces: 8. Diameter: 10 m. Separation: 25 m.	No trees
Num. 1	8,62	8,32	10,32	7,52	9,86	9,99	7,63	7,77	5,39
Num. 2	17,69	9,91	10,90	8,56	9,78	10,01	6,92	8,19	6,35
Num. 3	8,83	10,06	10,30	10,06	9,55	9,99	9,77	9,87	11,50
Num. 4	9,30	10,62	9,89	9,14	7,44	9,84	9,80	10,35	9,80
Num. 5	5,87	5,88	6,09	6,21	6,38	5,54	5,77	5,49	4,20
Num. 6	8,25	7,59	8,43	9,54	7,85	8,22	8,90	8,55	11,67
Num. 7	6,87	6,45	7,25	6,19	4,51	5,24	6,20	4,61	9,24
Num. 8	7,74	8,37	9,44	10,05	6,12	6,76	8,85	9,52	8,55
Num. 9	5,85	9,10	10,56	9,86	11,13	9,27	9,70	10,22	6,67
Num. 10	8,95	7,96	9,92	12,95	8,54	6,51	7,83	11,45	11,55
Num. 11	8,33	7,82	8,00	8,94	9,97	8,72	9,41	10,00	11,03
Num. 12	5,27	5,95	5,69	7,84	4,02	7,52	5,38	4,84	9,06
Num. 13	12,37	11,84	14,40	15,98	12,90	12,79	14,49	14,62	9,57
Num. 14	1,69	3,60	4,45	3,53	2,05	1,96	2,34	4,98	3,70
Num. 15	9,59	10,63	12,37	9,77	8,43	10,72	9,36	9,23	13,87
Num. 16	1,56	10,99	12,59	10,27	NaN	1,98	13,06	9,23	2,20
Num. 17	9,70	7,56	10,25	9,56	3,65	7,70	9,80	11,70	14,97
Num. 18	NaN	NaN	NaN	NaN	NaN	NaN	NaN	NaN	NaN
Num. 19	7,29	7,82	8,73	9,87	5,74	4,50	7,92	7,15	13,10
Num. 20	NaN	NaN	NaN	NaN	NaN	NaN	NaN	NaN	NaN

Bibliography

[1] Ian Poole. *Radio and Communications Technology*. Newnes, 2003.

[2] Allan W. Scott and Rex Frobenius. *RF Measurements for Cellular Phones and Wireless data systems*. Wiley, 2008.

[3] Paul G. Hurayg. *Maxwell's Equations*. Wiley-IEEE, 2009.

[4] Paul G. Hurayg. *Propagation of radiowaves. 2nd Edition*. Les Barclay, 2003.

[5] Paul A. Tipler and Gene Mosca. *Fsica. Para la ciencia y la tecnologa*. Editorial Revert, 2005.

[6] Oliver Bouchet, Herve Sizun, and Christian Boisrobert. *Free-Space Optics. Propagation and communication*. Iste, 2004.

[7] H. Sizun. *Radio Wave Propagation for Telecommunication Applications*. Springer, 2003.

[8] Thomas Kurner. Planning of terrestrial radio networks. 2009.

[9] Jürgen Richter, Rafael F. S. Caldeirinha, and Miqdad O. Al-Nuaimi. A generic narrowband model for radiowave propagation through vegetation. 2005.

[10] J.D. Parsons. *The mobile Radio Propagation Channel*. John Wiley & sons LTD, 2000.

[11] Wang Chao and ZHANG Hong. The scattering study of rough surface by ray tracing technique. *Internation Conference on Environmental Science and Information Application Technology*, pages 704–707, 2009.

[12] Jong Yvo L.C. de. Measurement and modelling of radiowave propagation in urban microcells. *CIP-DATA LIBRARY TECHNISCHE UNIVERSITEIT EINDHOVEN*, 2001.

[13] Saúl A. Torrico, Henry L. Bertoni, and Roger H. Lang. Modeling tree effects on path loss in a residential environment. *IEEE Transactions on Antennas and propagation*, 46(6):872–880, 1998.

[14] V.S. Abhayawardhana, I.J. Wassell, D. Crosby, M.P. Sellars, and M.G. Brown. Comparison of empirical propagation path loss models for fixed wireless access systems. *61th IEEE Technology Conference, Stockholm*, 2005.

[15] International Telecommunication Union. Recommendation itu-r p.833-5, attenuation in vegetation. *Tech. Rep. P.833-2*, 2001.

[16] Spectrum Engineering Advanced Monte Carlo Analysis Tool. Seamcat. `http://www.seamcat.org`, 2010. [Online; March 21-March-2011].

[17] Jong Yvo L.C. de and Matti H. A. J. Herben. A tree-scattering model for improved propagation prediction in urban microcells. *IEEE Transactions on vehicular technology*, 53(2), 2004.

[18] Saúl A. Torrico and Roger H. Lang. A simplified analytical model to predict the specific attenuation of a tree canopy. *IEEE Transactions on Antennas and propagation*, 56(2):696–703, 2007.

[19] American Forests. Americanforests. `http://www.americanforests.org`, 2010. [Online; accessed 22-October-2010].

[20] Boris Zeide. How to measure stand density. *TREES - STRUCTURE AND FUNCTION*, 19(1,1-14), 2003.

[21] R. Hedl, M. Svatek, M. Dancak, Rodzay A.W., M. Salleh A.B., and Kamariah A.S. A new technique for inventory of permanent plots in tropical forests. *ingentaconnect.com*, pages 124–120, 2009.

[22] John D. Shaw. Reinekes stand density index: Where are we and where do we go from here? *USDA Forest Service, Rocky Mountain Research Station*, 2005.

[23] W. Liu, Y. Du, Q. Sun, Z. Yan, and I. Wu. Analyis of insar sensitivity to forest structure based in radar scattering model. *Progress In Electromagnetics Research*, 2008.

[24] Tung Tsang. *Classical electrodynamics*. World Scientific Publishing Co., 1997.

[25] Josep Burillo, Alcia Miralles, and Oriol Serra. *Propabilitat i estadstica*. Edicions UPC, 2003.

[26] Yu Song Meng, Yee Hui Lee, and Boon Chong Ng. Empirical near ground path loss modeling in a forest at vhf and uhf bands. *IEEE Transactions on antennas and propagation*, 57(5), 2009.

[27] John G. Grimes. Global positioning system standard positioning service performance standard. 2008.

[28] Felix K. Schwering, Edmond J. Violette, and Richard H. Espeland. Millimeter-wave propagation in vegetation: Experiments and theory. *IEEE Transactions on geoscience and remote sensing*, 26(3), 1988.

[29] Inc WiMax.com Broadband Solutions. WiMax.com 4G Wireless Broadband Solutions. `http://www.wimax.com`, 2010. [Online; accessed 19-October-2010].

[30] International Telecommunications Union. Itu. `http://www.itu.int`, 2010. [Online; accessed 04-November-2010].

[31] European Telecommunications Standards Institute. Etsi. `http://www.etsi.org`, 2010. [Online; accessed 04-November-2010].

[32] European Conference of Postal and Telecommunications Administrations. Cept. `http://www.cept.org`, 2010. [Online; accessed 04-November-2010].

[33] International Telecomunication Union. *Radio Regulations*. ITU, Geneva 1998.

[34] Dayan Adionel Guimares. *Digital Transmission*. Springer, 2010.

[35] David J. Withers. *Radio Spectrum Management*. The Institution of Electrical Engineers, 1999.

[36] Akira Ishimaru. *Wave Propagation and Scattering in Random Media*. IEEE PRESS, 1997.

[37] Latex. Latex project. `http://www.latex-project.org`, 2010. [Online; accessed 25-September-2010].

[38] Matlab. Mathworks. accelerating the pace of engineering and science. `http://www.mathworks.com`, 2010. [Online; accessed 25-September-2010].